

THE ELECTROMAGNETIC SEPARATORS IN NUCLEAR PHYSICS

BERTRAND JACQUOT
GANIL, France

Abstract:

In this lecture, we give an overview of the variety of electromagnetic spectrometers and separators used in nuclear physics. Some important notions of charged particles optics are introduced. Then, we present the different spectrometers which are used at present in nuclear physics laboratories, depending on the energy domain. We conclude this document with some practical details about the tuning of the spectrometers and associated diagnostics.

- 1. INTRODUCTION

Why separator and/or spectrometer?

- 2. BASIC NOTIONS IN CHARGED PARTICLE OPTICS

$B\rho$, Transport matrix, quadrupole gradients

- 3. SPECTROMETERS AROUND THE COULOMB BARRIER

RMS, gas filled separator, large acceptance spectrometer

- 4. SEPARATORS AT HIGH ENERGY

Fragment separators, high energy spectrometer

- 5. SPECTROMETER TUNING AND DIAGNOSTICS

Profil measurement, dipole & quadrupole tuning, alignment

- 6. CONCLUSION

APPENDIX:

LISE++ simulation code

Numerical integration of the equations of motion

The quadrupole matrix

Ion stripping in solid targets

Wedge shape of the degrader

Emittance evolution in a beam line

Focusing in bending magnets

1. INTRODUCTION

We overview in this lecture the different techniques used to purify and analyze the nuclear reaction products with magnetic fields [MUN92]. We exclude from this document the ion traps, used especially for high-resolution mass measurements, calorimeters and detectors used in high-energy accelerators and colliders (for example Alice at LHC, Hades at GSI).

The developments of accelerators, detectors and spectrometers enriched the field of nuclear physics.

During the last years, separators and spectrometers have had to adapt themselves to recent advances in detection methods and accelerators. They must ensure selection and /or identification of the reaction products with the best possible efficiency, while rejecting the flow of the unwanted ions.

The experimentalist faces a general question to measure a given observable:

Is a spectrometer really needed for my specific experiment?

A lot of wonderful results have been indeed obtained without any spectrometer. A global answer is that the spectrometer boosts **the selectivity** of any experiment: that is to say the ability to select rare events with a huge amount of unwanted events. Besides an electromagnetic spectrometer can provide **the identification** of the ions produced in nuclear reactions events by events. However since the spectrometer transmission is sometimes very low, it is important to evaluate the advantages versus the main drawback (the low efficiency).

Two functions are clearly distinguished: the separator function (elimination of the primary beam) and the spectrometer function (measurement of $B\rho$, or Energy, Velocity,...)

In the following, I will mainly present electromagnetic devices that can provide the two functions. The name given, separator or spectrometer, is related to the function considered as the most important one...

1.1 Separator (rejection of primary beam)

The separator's function is the elimination of a part of unwanted events and the selection of the desired events. This function is directly related to the technical limitations of the detection, which is not capable in most cases to process an event rate higher than 10^3 - 10^5 Hz. The particle's rate produced by the interaction of a beam of a modern ion accelerator (often capable of delivering 10^{12} à 10^{14} ions per second) with a solid target with is much larger than the detector's limitation.

Therefore the minimum function for a separator is the rejection (removal) of the most abundant particles, i.e. the ones of the primary beam. The elimination of other types of particles (coming from other reaction channels) is useful or necessary depending on the number of ions and the detection. This rejection's function of the unwanted events is of paramount importance in the study of rare events.

Rejection = number of unwanted events (primary beam) / detected events
= primary beam intensity on target / ion detector rate

For instance, the separators dedicated for the superheavy element synthesis (SHIP@Darmstadt, DG_FRS@Dubna, RITU@Jysvakyala ...) use generally a beam with 10^{12} particle per second (pps) on target. They eliminate most of the particle beam to get only 100 Hz on a silicon detector. It represents a rejection of 10^{10} . While the desired events represent often less than 0.01 Hz.

The detection must be the selective enough to distinguish the desired events among all the detected events.

1.2 Spectrometer

This function combines the properties of a separator with a detection system. A spectrometer is a separator used to measure a physical observable:

Electromagnetic separator + detector = spectrometer

The selection of certain ions depends on the technique used: either a magnetic separation or an electrostatic one. The resolution is the parameter to judge the quality of the overall analysis. The electromagnetic spectrometers do not measure directly the mass, A, Z, charge, or energy independently: most of the time, it is necessary to correlate multiple parameters to clearly identify an ion or measuring a characteristic of interest:

Often, it relies on two measurements as we will see later in this lecture

- a **velocity** measurement (v) given by a Time-of-Flight: $v=L / \text{ToF}$
- a **magnetic rigidity** ($B\rho$) measurement given by a position: $B \sim A/Qv$

The identification starts with the computation of the "A/Q" value, associated to the detected ion:

$$A/Q \sim [B\rho/v]$$

2. BASIC NOTIONS IN CHARGED PARTICLE OPTICS

2.1 Ion beams

2.1.1 Ion beams provided by an accelerator

The charged particles delivered by an accelerator circulate in stainless steel tubes (vacuum chambers). They rarely occupy more than a few tenth of mm^2 in the center of the vacuum chambers. These particles have low velocity dispersion ($\Delta v/v < 1\%$) and very low relative angle (< 10 mrad). We speak about particle beams just, as one speaks of the light beam. Individually particles oscillate around the ideal line along the laboratory beam lines (the vacuum chambers center represents the reference trajectory).

The discontinuous time structure of the accelerated ion beam

At the exit of an Radio-Frequency accelerator (cyclotron, linac, synchrotron), the particles arrive in bunches separated by few nanoseconds. This time structure is related to the acceleration with alternating electric fields (RF).

But, in electrostatic accelerator, like Van de Graff accelerators, the beams are continuous, because this type of accelerator uses static electric fields.

For particles coordinates, we use a curvilinear coordinate system (x, y, s), whose reference is the center of the vacuum chamber along the beam lines.

2.1.2 The magnetic rigidity: The “Bρ” (Tesla.m)

A charged particle (M, q, v) moving in a field B (magnetic induction) uniform and transverse ($\mathbf{v} \perp \mathbf{B}$), follows a circular path. The radius of curvature of an ion is determined by the equilibrium of the centrifugal force and the Lorentz force:

$$\frac{d\mathbf{p}}{dt} = \mathbf{F} = q(\mathbf{v} \times \mathbf{B}) \quad \text{With } \mathbf{p} = \gamma M \mathbf{v}$$

Where ($\mathbf{v} \perp \mathbf{F}$), hence the modulus $|\mathbf{v}| = \text{Constant}$ and $\gamma = \text{constant}$

The motion is circular and uniform: $\frac{d\mathbf{v}}{dt} = \frac{|\mathbf{v}|^2}{R} e_r$ and so $\gamma M v^2 / R = q |\mathbf{v}| |\mathbf{B}|$

$$\text{The curvature radius of the trajectory is then } R = \frac{\gamma m v}{q B}$$

We define the magnetic rigidity Bρ, as the main characteristics of a given ion (M, q, v): it permits to know the radius of the trajectory in a constant B field.

$$B\rho = \frac{\gamma M v}{q} = \frac{P}{q}$$

Indeed, this important parameter allows the setting of a magnetic spectrometer, since we adjust the B_{dipole} field of a magnetic dipole (having a reference radius of curvature R_{dipole}) to select particles having a given magnetic rigidity (Bρ) with the simple equation:

$$B_{\text{dipole}} = B\rho / R_{\text{dipole}}$$

The knowledge of the “Bρ” is the only information required to guide an ion in a magnetic spectrometer. Moreover it is more convenient to use a parameter which unit is simpler and convenient compared to that of triplet [M, q, v] expressed in a unit system not really adapted [MeV/c², Coulomb, cm/ns] to the evaluation of dipole magnetic field in Tesla.

Numerical example:

A carbon ion beam ¹²C⁶⁺ having a kinetic energy of 47.05 MeV/A (E=564.65 MeV), has a magnetic rigidity of 2.0 T.m. A magnetic dipole with a bending angle φ=45° and a reference curvature radius R_{dipole}=3.0m, has to be tuned at B=0.6666 Tesla. With such a field the ion deflection will really be 45°.

2.1.3 The electric rigidity: The “Eρ” (in Volt or MVolt)

This “Eρ” is useful in spectrometers with electrostatic elements. A charged particle (M, q) moving in an electric field E follows a circular path, if the electric field is perpendicular to the velocity at any point. This is accomplished in electrostatic dipoles of some spectrometers. The radius of curvature R of the path in a transverse E, field is calculated as before:

$$\frac{d\mathbf{p}}{dt} = \mathbf{F} = q \mathbf{E}, \text{ if } (\mathbf{v} \perp \mathbf{E}) \Rightarrow |\mathbf{v}| = \text{Constante et } \gamma = \text{constante}$$

$$\text{So } \frac{d\mathbf{v}}{dt} = \frac{|\mathbf{v}|^2}{R} e_r, \text{ which leads to } \gamma M v^2 / R = q |\mathbf{E}| \quad R = \frac{\gamma M v^2}{q E}$$

We define, the electrical rigidity Eρ: It is the parameter that allows you to know the radius of curvature of a particle in an electric dipole:

$$E\rho = \gamma M v^2 / Q$$

This value permit to set the “E field” of a electric dipole (having a radius of curvature R_{E dipole}) to select particles with a magnetic rigidity (given Eρ):

$$: \quad E = E\rho / R_{\text{E dipole}}$$

Numerical example: A beam of $^{105}\text{Sn}^{20+}$ travelling at 1.0 MeV/A ($E=105 \text{ MeV} \sim Mv^2/2$) has an electric rigidity $E_p=10\text{MV}$. Electric fields are not used with high-energy particles, since the required electrical field is not technologically achievable (the required electric field strength evolves as v^2). The magnetic bending forces are more effective because they are proportional to the velocity ($F=qvB$) while the electric force is just proportional to the applied field: $F=qE$

2.2 The components of a spectrometer

2.2.1 Magnetic dipoles

Magnetic dipoles are electromagnets. They have coils and two poles which guide the field lines. They allow obtaining a uniform vertical magnetic field.

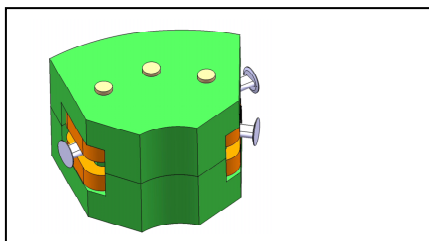


Figure 1a: Base component of a spectrometer, the magnetic dipole:

It allows to bend the ion trajectory and select ions with a given magnetic rigidity.

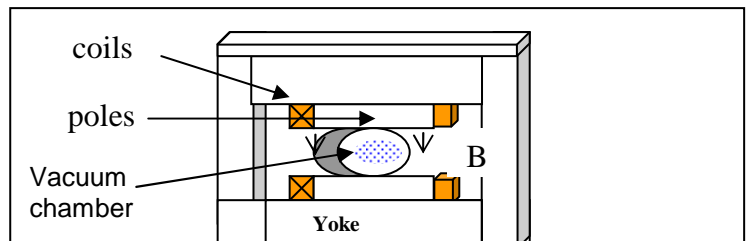


Figure 1b : Sectional view of a magnetic dipole (model H). The calculation of the field B depends on the current I in the coils and the gap g between the poles. : $B \sim I / g$. With iron poles, it is difficult to reach higher fields than $B = 1.6$ Tesla which corresponds to the saturation of the iron poles.

2.2.2 Magnetic quadrupoles

Such an electromagnet is used to focus the beam. The quadrupole can avoid particle losses on the edges of the vacuum chambers of the beam lines. The quadrupole focuses horizontally and defocuses vertically (or vice versa). The forces experienced by particles are proportional to their position (x, y).

For instance, if the vertical field is $B_y=Gx$, it produces an horizontal force $F_x \sim G x$, where G is called the “**quadrupole Gradient**” (since $B_y=Gx$, we have $G=dB_y/dx$).

The focusing strength of a quadrupole having a length L_q and gradient G also depends on the magnetic rigidity of the beam:

$$\text{Horizontal Force } F_x = q (\mathbf{v} \times \mathbf{B})_x = q \cdot v_z \cdot B_y = q v_z \cdot G \cdot x$$

$$F_x \sim + x \cdot G$$

$$\text{quadrupole effect in } x \sim + xG L_q / B\rho$$

$$\text{Vertical Force } F_y \sim - y \cdot G$$

$$\text{quadrupole effect in } y \sim - yG L_q / B\rho$$

A set of quadrupole helps to focus the beam in the following locations:

- Output of a spectrometer to optimize the resolution of the spectrometer
- Before the reaction target of a spectrometer to optimize the optical quality of the product ion beams in reaction
- Interaction area of a particle collider to increase brightness [high energy physics]

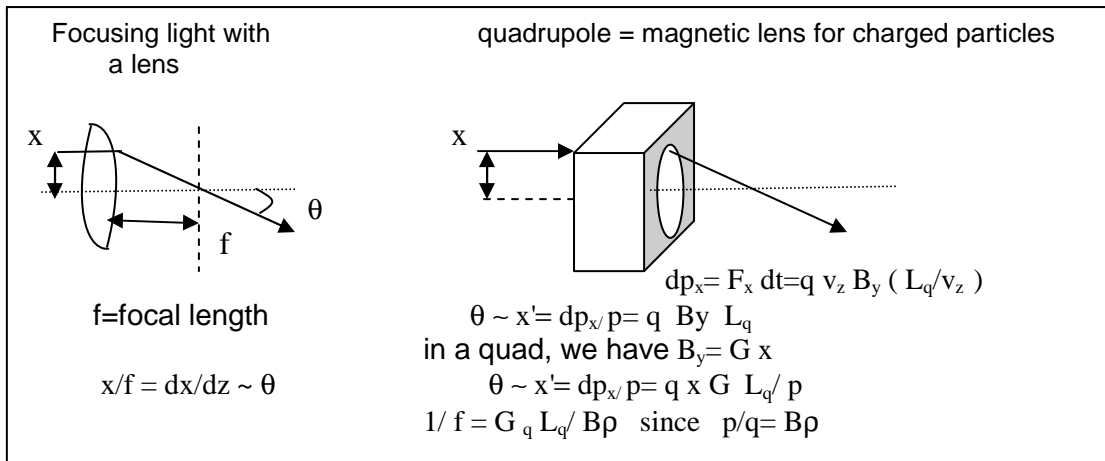
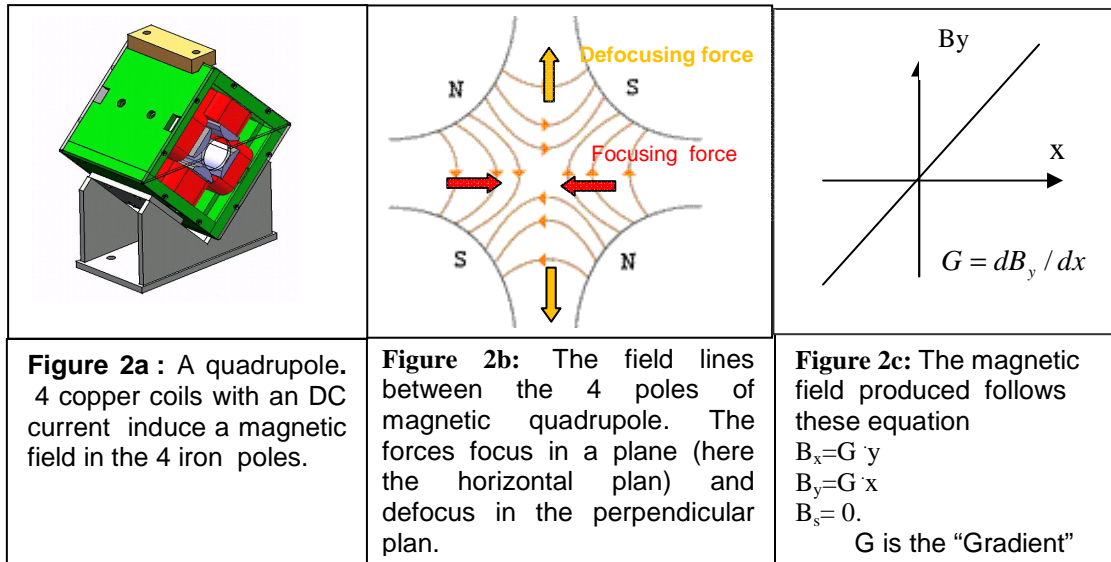


Figure 3: Comparison between a optical lens and quadrupole which is an ion lens.

A quadrupole combination with alternating polarities (focusing and defocusing) can be used to focus a particle beam in the two directions (horizontal and vertical).

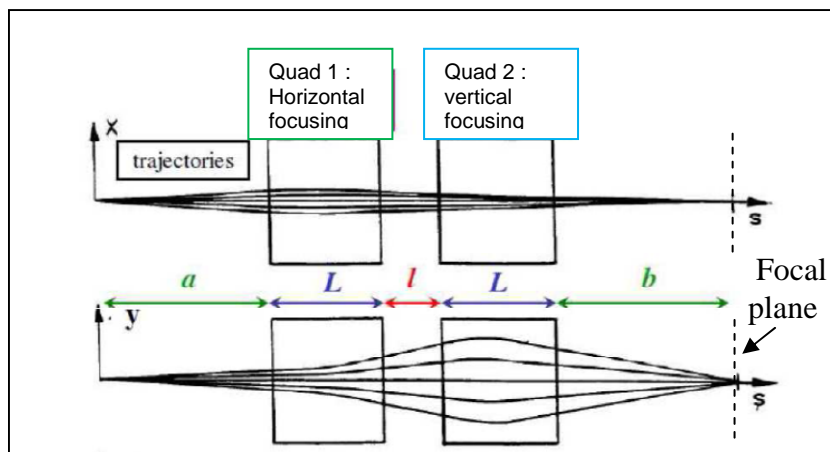


Figure 4: transport of 5 trajectories in 2 quadrupoles: The net effect is focusing in horizontal (x) and vertical (y) directions, if the gradients (G_{q1}, G_{q2}) are properly chosen...

2.2.3 Drift length: the space without magnet

The space between two electromagnets is called "DRIFT". The length between the magnets is optimized to obtain the best performance for the spectrometer (focusing, angular acceptance and resolution).

2.3 Charged particle optics

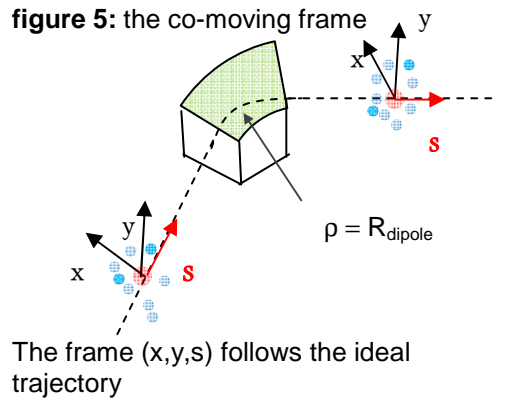
2.3.1 Equation of motion

Particle dynamics is calculated using the "Newton-Lorentz" equation:

$$\frac{d}{dt}[m\gamma \mathbf{v}] = q \cdot (\mathbf{E} + \mathbf{v} \times \mathbf{B})$$

We seek to express how the coordinates of a particle evolves along a spectrometer in the reference frame which follows the reference particle. This reference frame (x, y, s) is a co-moving orthogonal, and right-handed coordinate system.

Locally, in a dipole magnet with a curvature radius ρ , the equations in the magnetic fields appear as follows:

$\frac{dx}{ds} = x'$ $\frac{dy}{ds} = y'$ $\frac{d}{ds} \left[m\gamma \dot{x} \right] = m\gamma \dot{s} \left(1 + \frac{x}{\rho} \right) + q \left(+y' B_s - \dot{s} \left(1 + \frac{x}{\rho} \right) \cdot B_y \right)$ $\frac{d}{ds} \left[m\gamma \dot{y} \right] = q \left(\left(1 + \frac{x}{\rho} \right) \cdot B_x - x' \cdot B_s \right)$ $\frac{d}{ds} \left[m\gamma \dot{s} \left(1 + \frac{x}{\rho} \right) \right] = -\frac{m\gamma \dot{x}}{\rho} + q \left(x' \cdot B_y - y' \cdot B_x \right)$	<p>figure 5: the co-moving frame</p>  <p>The frame (x,y,s) follows the ideal trajectory</p> <p><u>The curvature ρ of the frame:</u> in a dipole magnet $\rho = R_{\text{dipole}} = \Delta\phi / L$ in a drift or a quad $\rho = \infty$</p>
---	---

To simulate the trajectories of charged particles, we must proceed as follows

- 1) We must know B (x, y, z) for each optical element [3 dimensional field maps]
- 2) We must Integrate the equations of motion numerically with a "Euler" or "Runge-Kutta" algorithm for each particle using the field maps (see APPENDIX 2)

This approach is time consuming and often unnecessary, as there is a simplified approach: the matrix approach.

2.3.2 Particle coordinates

We use the curvilinear frame (x, y, s) which follows the ideal path of the beam line to describe the particle coordinates.

At any specified longitudinal position s in the spectrometer, a charged particle is represented by a vector \mathbf{Z} , whose components are the positions, angles, and magnetic rigidity of the particle with respect to the reference trajectory

The coordinates are written as follows: $\mathbf{Z} = (x, x', y, y', l, \delta)_s$

- x and y are the transverse coordinates of the center of the vacuum chamber
 - x' et y' a related to the horizontal and vertical angles with respect to the reference axis
- For a particle, we have the following relationship:

$$\tan \theta = dx/ds = x' \quad \text{and} \quad \tan \phi = dy/ds = y'$$

- $l = s - s_0 = v_0 (t - t_0)$ is the difference in longitudinal position relative to the reference particle.
- $\delta = (B\rho - B\rho_0) / B\rho_0$ Relative difference in rigidity compared to the reference particle.

The reference particle has the coordinate $\mathbf{Z} = (0, 0, 0, 0, 0, 0)_s$

The computation of the evolution of particle from a point A to B can be written as follow

$$\mathbf{Z}(s_B) = \mathbf{M}(\mathbf{Z}(s_A), \mathbf{B}) \text{ where } \mathbf{M} \text{ is the transfer function}$$

2.3.3 Beam optics with first order approximations

We can perform a development of the equations of motion for a trajectory close to the reference path and, then by truncating the Taylor expansion to the first order in $(\Delta x, \Delta x', \Delta y, \dots)$. The final position of a particle at the end of the spectrometer will depends linearly on the initial coordinates.

$$\mathbf{Z}(s_B) = \mathbf{M}(\mathbf{Z}(s_A), \mathbf{B}) = \mathbf{R}(\mathbf{B} \dots) \cdot \mathbf{Z}(s_B) + 0(\mathbf{Z}^2)$$

↑ **First order** ↙ **higher orders neglected**

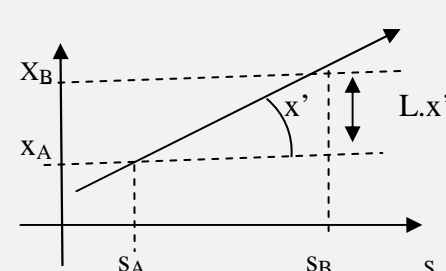
The relationship between entrance & exit coordinates is stored in a matrix called "transfer matrix". This matrix R permits to calculate, easily, the coordinates of a particle at the end of a spectrometer, knowing its initial coordinates.

- $\mathbf{Z}_A = (x, x', y, y', l, \delta)_A$ initial coordinates (at the target generally)
- $\mathbf{Z}_B = (x, x', y, y', l, \delta)_B$ final coordinates (final detector position)

$$\mathbf{Z}_B = \mathbf{R} \cdot \mathbf{Z}_A$$

$$\begin{bmatrix} x \\ x' \\ y \\ y' \\ l \\ \delta \end{bmatrix}_B = \begin{bmatrix} R_{11} & R_{12} & R_{13} & R_{14} & R_{15} & R_{16} \\ R_{21} & R_{22} & R_{23} & R_{24} & R_{25} & R_{26} \\ R_{31} & R_{32} & R_{33} & R_{34} & R_{35} & R_{36} \\ R_{41} & R_{42} & R_{43} & R_{44} & R_{45} & R_{46} \\ R_{51} & R_{52} & R_{53} & R_{54} & R_{55} & R_{56} \\ R_{61} & R_{62} & R_{63} & R_{64} & R_{65} & R_{66} \end{bmatrix} \begin{bmatrix} x \\ x' \\ y \\ y' \\ l \\ \delta \end{bmatrix}_A$$

$l = v_0(t - t_0)$
 $\delta = \frac{B\rho - B\rho_0}{B\rho_0}$

<p>Exercise A: How to represent an ion drift following a straight line with the matrix coefficients?</p> 	<p>Answer: The beam dynamic without magnetic field is simple. Starting from the initial position x_A, the final position x_B after a drift length L can be computed easily:</p> $x_B = x_A + (s_B - s_A) dx_A/ds = x_A + L x'_A$ <p>The final position after a drift is represented with the matrix approach as: $\mathbf{Z}_B = \mathbf{R} \cdot \mathbf{Z}_A$, so in the horizontal plane</p> $x_B = R_{11} x_A + R_{12} x'_A$ <p>so for a drift length L, $R_{11}=1$ and $R_{12}=L$</p>
---	--

The matrix interpretation:

The R_{ij} matrix coefficients are the partial derivatives of the final coordinates as a function of the initial coordinates.

$$R_{ij} = \left(\frac{\partial Z_{Bi}}{\partial Z_{Aj}} \right)$$

$$ex: \quad R_{11} = \left(\frac{\partial Z_{B1}}{\partial Z_{A1}} \right) = \left(\frac{\partial x_B}{\partial x_A} \right) \quad R_{12} = \left(\frac{\partial Z_{B1}}{\partial Z_{A2}} \right) = \left(\frac{\partial x_B}{\partial x'_A} \right)$$

$$R_{16} = \left(\frac{\partial Z_{B1}}{\partial Z_{A6}} \right) = \left(\frac{\partial x_B}{\partial \delta_A} \right)$$

To make obvious the meaning of the matrix elements, some authors write the matrix elements as follows:

$$R_{16} = (x | \delta); \quad R_{11} = (x | x) \\ R_{12} = (x | x'); \quad R_{34} = (y | y') \text{ etc....}$$

Remember that x' is related to the horizontal angle: $x' = \tan \theta \sim \theta$

For a beam line section which consists of a quadrupole q_1 , a drift length L and a quadrupole q_2 , the total transfer matrix of the section is the product of the transfer matrices:

$$\mathbf{R}(q_1, L, q_2) = \mathbf{R}(q_2) \cdot \mathbf{R}(L) \cdot \mathbf{R}(q_1) \\ (\text{Pay attention to the order, since the product is non commutative})$$

The transport matrix R depends on

- The geometry of the spectrometer (distances, deviation angle)
- The quadrupoles settings (the gradients G , where $G = dB_y/dx$ for each quadrupole)

The properties of a spectrometer in most cases are given below:

A) It starts with a focus and ends up in a focus point ($R_{12} = R_{34} = 0$ conditions that correspond to a "point-to-point focusing")

B) The spectrometer is dispersive ($R_{16} \neq 0$)

The global spectrometer matrix takes the following form:

See the next exercise.

$$\begin{bmatrix} x \\ x' \\ y \\ y' \\ l \\ \delta \end{bmatrix}_1 = \begin{bmatrix} R_{11} & 0 & 0 & 0 & 0 & R_{16} \\ R_{21} & R_{22} & 0 & 0 & 0 & R_{26} \\ 0 & 0 & R_{33} & 0 & 0 & 0 \\ 0 & 0 & R_{43} & R_{44} & 0 & 0 \\ 0 & 0 & 0 & 0 & 1 & L/\gamma^2 \\ 0 & 0 & 0 & 0 & 0 & 1 \end{bmatrix} \begin{bmatrix} x \\ x' \\ y \\ y' \\ l \\ \delta \end{bmatrix}_0 \quad \begin{matrix} l = v_0(t - t_0) \\ \delta = \frac{B\rho - B\rho_0}{B\rho_0} \end{matrix}$$

With such a matrix, for an ion having the initial coordinates $(x_0, x'_0, y_0, y'_0, l_0, \delta_0)$, we compute its position x_1 in horizontal plane at the end of the spectrometer:

$$x_1 = R_{11} x_0 + R_{16} \delta_0 = R_{16} \delta_0 \quad (\text{we have used } Z_1 = R Z_0)$$

The knowledge of the dispersion $R_{16} = \partial x_1 / \partial \delta_0$ permits to predict the position x_1 in any spectrometer if δ_0 is known ...

Such a transport matrix indicates that the rigidity of the ions is not affected by the spectrometer:

$$\delta_1 = R_{61} x_0 + R_{62} x'_0 + R_{63} y_0 + R_{64} y'_0 + R_{65} l_0 + R_{66} \delta_0 = \delta_0$$

$$\text{So } B\rho_1 = B\rho_{\text{ref}} (1 + \delta_1) = B\rho_{\text{ref}} (1 + \delta_0) = B\rho_0$$

The optical matrix method, called "first order optics", is an approximation but this is the basic approach for the understanding of the main optical properties of any spectrometer.

Exercise B: Demonstrate that the relationship between the final particle position x_1 , of an ion, and its magnetic rigidity is:

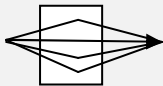
$$B\rho = B\rho_{\text{ref}} (1 + x_1/R_{16})$$

Answer: using the matrix equation $Z_1 = R Z_0$, The final position will depend on all the initial coordinates:

$$x_1 = R_{11} x_0 + R_{12} x'_0 + R_{13} y_0 + R_{14} y'_0 + R_{15} l_0 + R_{16} \delta_0$$

We demonstrate here why most of the coefficients are zero in spectrometer

- a) if the beam is focused at the entrance of the spectrometer $x_0 \sim 0$
- b) if the final position at the exit of the spectrometer (detector position) is located at the focus, (where all particles are focused whatever the initial horizontal angle x'_0)



$$R_{12} = \left(\frac{\partial x_1}{\partial x'_0} \right) = 0$$

(point to point focusing: final position x_1 independent from the initial angle x'_0)

- c) The quadrupoles create a force F_x in the horizontal plane which is independent from the vertical position y or angle y' ($F_x = q v_z \cdot G \cdot x$), and it is the same for dipole magnet (where $F_x = q v_z \cdot B_0$), so

$$R_{13} = \left(\frac{\partial x_1}{\partial y_0} \right) = 0 \quad \text{and} \quad R_{14} = \left(\frac{\partial x_1}{\partial y'_0} \right) = 0$$

- c) a spectrometer uses static magnetic fields, so the final position is independent from the time so

$$R_{15} = \left(\frac{\partial x_1}{\partial t} \right) = \left(\frac{\partial x_1}{\partial l_0} \right) = 0$$

finally (b+c) \Rightarrow

$$\begin{aligned} x_1 &= R_{11} x_0 + R_{12} x'_0 + R_{13} y_0 + R_{14} y'_0 + R_{15} l_0 + R_{16} \delta_0 \\ &= R_{11} x_0 + R_{16} \delta_0 \\ &\sim R_{16} \delta_0 \quad \text{since } x_0 \sim 0 \quad (\text{a}) \end{aligned}$$

So if you know R_{16} , the measurement of x_1 allows the computation of the $B\rho$ deviation δ_0
 $\delta_0 \sim x_1/R_{16}$ (we have assume that $x_0=0$).

Since $B\rho = B\rho_{\text{ref}}(1 + \delta_0)$, we have

$$\begin{aligned} \delta_0 &= [B\rho - B\rho_{\text{ref}}] / B\rho_{\text{ref}} = x_1/R_{16} \\ \text{so} \quad B\rho &= B\rho_{\text{ref}} (1 + x_1 / R_{16}) \end{aligned}$$

Nota: if the beam size at the entrance of the spectrometer is Δx_0 , the measurement error is related to $R_{11} \Delta x_0 / R_{16}$ since: $\delta_0 = x_1 / R_{16} \pm R_{11} \Delta x_0 / R_{16}$
 The error of the $B\rho$ measurement ($\delta_0 \pm R_{11} \Delta x_0 / R_{16}$) is related to the spectrometer resolution.

2.3.4 Spectrometer resolution

The resolution of a magnetic spectrometer is defined as the difference necessary to distinguish 2 beams with a size σ_{x_1} at the focal plane:

$$\text{Resolution "FWHM"} = R_{\text{FWHM}} = 2.35 \sigma_{x_1} / R_{16}$$

where $R_{16} = (x / \delta)$ is the spectrometer dispersion

Nota: This FWHM resolution correspond the a separation of the two beam at the half height. Sometimes for a separator, the resolution is defined with more constraints:

$$R_{\text{separation}} = 4 \sigma_{x1} / R_{16}$$

This “separation resolution” corresponds to the separation at the base of the gaussian ion beam.

Numerical example: A separator having a dispersion $R_{16}=2 \text{ m}$ ($=2\text{cm}/\%$) and $\sigma_x=0.5 \text{ mm}$, possesses a resolution $R_{\text{separation}}=1/1000$ in $B\rho$

2.3.5 Angular acceptance for a spectrometer

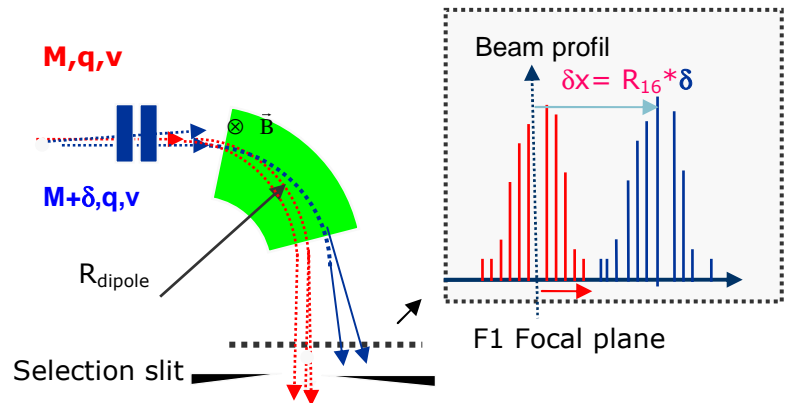
Figure 6: Separation of 2 particle beams, with a relative mass difference δ . The beams are well separated if:

$$R_{16} \times \delta > 4 \sigma_{x1}$$

At the selection point, we place selection slits and a position sensitive detector.

At the 1st order, the beam size σ_{x1} is related to the beam size at the entrance of the spectrometer:

$$\sigma_{x1} = R_{11} \sigma_{x0} + \dots$$



Behind a reaction target, nuclear fragments can be emitted in an emission cone having a large solid angle (expressed in steradian). It is sometimes very difficult for a quadrupole set to recover all the fragments. The efficiency of the spectrometer can be low because of these beam losses.

The **angular acceptance** is the solid angle that the spectrometer is able to recover after the reaction target:

$$d\Omega(\text{strd}) = \frac{dS}{4\pi r^2}$$

Instead of $d\Omega$, the maximal angle (in milliradians) transmitted in the spectrometer are often presented:

Ex: “the Angular acceptance is $\pm 40 \text{ mrad}$ in the horizontal plane
 $\pm 45 \text{ mrd}$, in the vertical plane ”

Let us mention than the angular acceptance is generally given for the particles having the reference rigidity $B\rho_{\text{ref}}$.

The angular acceptance of a spectrometer can be increased, if the size of the quadrupoles are pushed to maximum (the aperture of the quadrupole will define the radius of the cylindrical vacuum chamber). Since the maximum magnetic field at the poles is limited ($B_{\text{poleMax}} \sim 1. \text{ T}$), with increasing radius, the magnetic field strength decreases.

Indeed, the maximum gradient decreases as $G_{\text{max}} = B_{\text{poleMax}} / R$ and the quadrupole is no longer adapted to high rigidity particles.

Therefore, in the spectrometer design, so there is a trade-off between angular acceptance and maximum magnetic rigidity $B\rho_{\text{max}}$.

Furthermore, increasing the acceptance of a spectrometer has important consequences: The increase of the quadrupole radius, air gaps of the dipoles, requires to

increase power supplies to achieve the same fields. Besides, the increase the volume of vacuum chamber requires to increase the pumping capacity of the vacuum system: finally there is an increase in the construction and operation budget.

2.3.6 The beam envelop and the beam ellipsoid

We consider a set of particles at the location s in beam line as a statistical set of points in the phase space. The mean values \bar{x} , \bar{y} (beam center) are not sufficient to describe the beam. The widths are as well fundamental parameters for each dimension (x, y, \dots).

The horizontal width σ_x , can be defined as a sum over the particles which compose the beam:

$$\sigma_x^2 = \sigma_{xx} = \sigma_{11} = \langle xx \rangle = \frac{1}{N} \sum_{\alpha=1, \dots, N} (x_\alpha - \bar{x}) \cdot (x_\alpha - \bar{x})$$

$\sigma_x = \sqrt{\sigma_{11}}$ is the RMS of the horizontal envelop.

Other interesting quantities are the angular width σ_{22} , and the correlation coefficient σ_{12} :

$$\sigma_{x'x'} = \sigma_{22} = \frac{1}{N} \sum_{\alpha} (x'_\alpha - \bar{x}') \cdot (x'_\alpha - \bar{x}') \quad \sigma_{xx'} = \sigma_{12} = \frac{1}{N} \sum_{\alpha} (x_\alpha - \bar{x}) \cdot (x'_\alpha - \bar{x}')$$

Let us represent a typical beam in the subspace $(x, \frac{dx}{ds}) = (x, x')$.

The distribution of the particle at the location s_0 allows to characterize the beam.

In the plane given by the position & the angle (x, x') , the beam appears to be an ellipse whose orientation is evolving along the beam lines. The variances $\sigma_{11}(s)$ and $\sigma_{22}(s)$ of the beam are related to the "x width" and "angular width" of the beam at a given point s in the beam line.

The ellipse equation is

$$\epsilon_x^2 = \sigma_{22}(s) x^2 + 2 \cdot \sigma_{12}(s) x x' + \sigma_{11}(s) x'^2$$

The ellipse area, called the (RMS) beam emittance, is a quantity which is conserved along the beam trajectory:

$$\begin{aligned} \text{Ellipse Area} = \text{Emittance} &= \pi \epsilon_x \\ &= \pi \sqrt{\sigma_{11}\sigma_{22} - \sigma_{12}\sigma_{21}} \end{aligned}$$

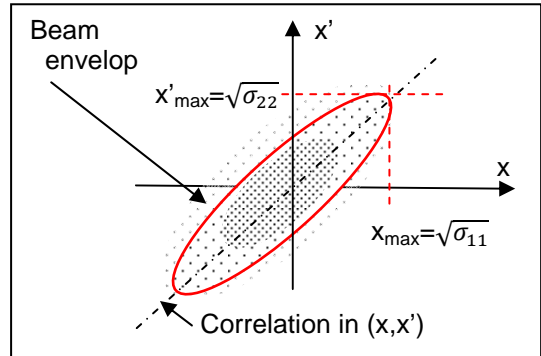


Figure 7: Typical beam distribution in the (x, x') plane. The inclination of the ellipse is related to the coefficient σ_{12} . For a focused beam, the ellipse is straight with no correlation between x and x' and $\sigma_{12}=0$. The normalized coefficient r_{12} is often used to describe the rotation of the beam ellipse $r_{12} = \sigma_{12} / \sqrt{\sigma_{11}\sigma_{22}}$

These quantities (σ_{11} , σ_{12} , σ_{22}) are generalized to the subspace (y, y') and (l, δ) . The beam matrix σ appears to be a 6x6 matrix:

$$\sigma(s) = \langle \mathbf{Z} \cdot \mathbf{Z}^T \rangle = \frac{1}{N} \sum_{\text{particles}} \begin{bmatrix} x \\ x' \\ y \\ y' \\ l \\ \delta \end{bmatrix} \cdot [x \quad x' \quad y \quad y' \quad l \quad \delta]$$

Generally, no correlation between the x and y planes exists, and the beam matrix σ possesses many zeros:

$$\sigma = \begin{pmatrix} \sigma_{11} & \sigma_{12} & 0 & 0 & 0 & \sigma_{11} \\ \sigma_{12} & \sigma_{22} & 0 & 0 & 0 & \sigma_{16} \\ 0 & 0 & \sigma_{33} & \sigma_{34} & 0 & 0 \\ 0 & 0 & \sigma_{43} & \sigma_{44} & 0 & 0 \\ \sigma_{51} & \sigma_{52} & 0 & 0 & \sigma_{55} & \sigma_{56} \\ 0 & 0 & 0 & 0 & \sigma_{65} & \sigma_{66} \end{pmatrix}$$

$$\text{With } \sigma_{ij} = \frac{1}{N} \sum_{\alpha} (Z_{\alpha}^i - \bar{Z}^i) \cdot (Z_{\alpha}^j - \bar{Z}^j)$$

$$\sigma_{11} = \langle x \cdot x \rangle = \frac{1}{N} \sum_{\alpha} x_{\alpha} \cdot x_{\alpha}$$

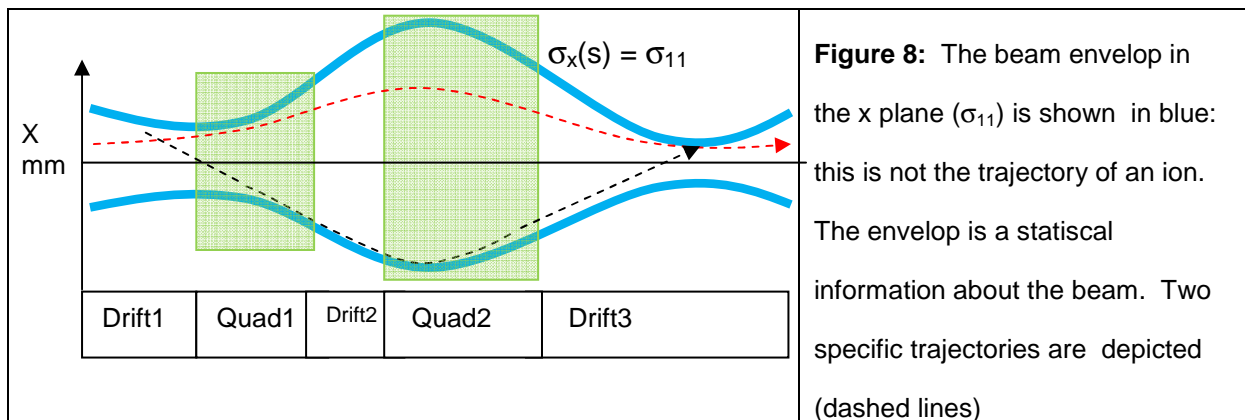
$$\sigma_{22} = \langle x' \cdot x' \rangle; \quad \sigma_{33} = \langle y \cdot y \rangle$$

No correlation for the beam between (y, y') and (x, x') because of the forces induced by the quadrupoles field ($F_x = G \cdot x, F_y = G \cdot y$): the forces in the horizontal plane, experienced by the particles are only correlated to the horizontal position in a quad....

The transformation of the beam matrix is given by the following relationship:

$$\sigma(s_2) = \langle \mathbf{Z} \cdot \mathbf{Z}^T(s_2) \rangle = \langle (R_{ik} \cdot Z_k(s_1)) \cdot (R_{jl} \cdot Z_l(s_1))^T \rangle$$

$$\sigma(s_2) = R(s_1 \rightarrow s_2) \cdot \sigma(s_1) \cdot R^T(s_1 \rightarrow s_2)$$



The transport matrix of the beam line depicted in figure 8 is the product of each element's matrix:

$$R = R_{\text{drift3}} \cdot R_{\text{quad2}} \cdot R_{\text{drift2}} \cdot R_{\text{quad1}} \cdot R_{\text{drift1}}$$

2.3.7 Optical simulations: how to compute the transport matrix?

The beam lines are designed for guiding the particle beam from one point to another: Many optical simulation codes are available on the Web (some are freeware) :

Transportgrafic, Mad, Transport 3rd order, Cosy infinity, Raytrace, TraceWin, GIOS ...

The simulation of a spectrometer with an optical matrix code is performed in different steps:

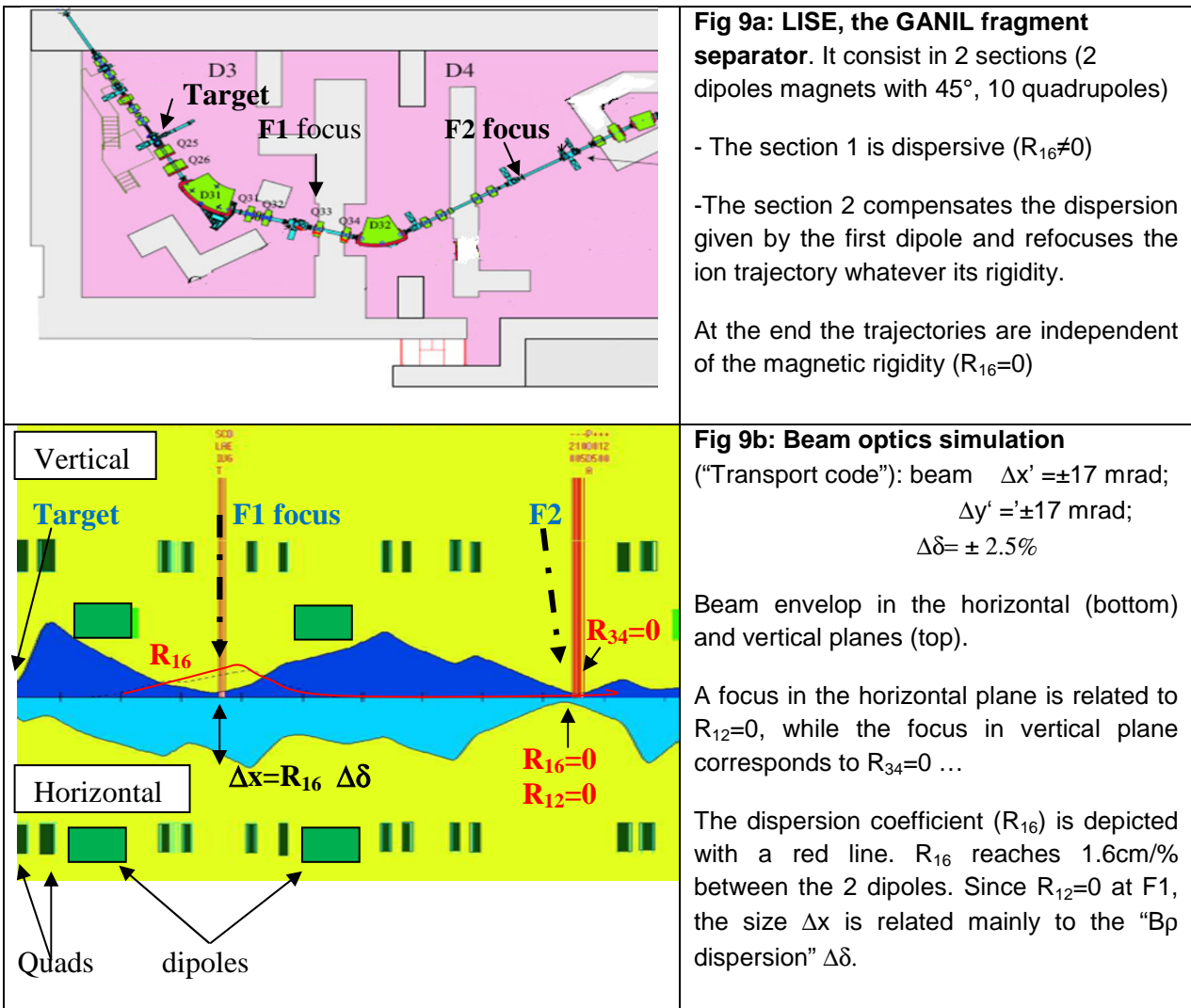
- Write the sequence of elements (type, length, gradient ...) in a definition file.

The optical program then calculates the global transfer matrix by multiplying the transfer matrices of each element (drift, dipole, quad ...).

- Change the quadrupole setting (gradients $G=dB_y/dx$) or change the spectrometer geometry (more quads...) if the beam envelop is not satisfactory.

Quadrupoles, dipoles and drift matrices are analytical and depend on the parameters of the elements (type, length, gradient, angle ...). There are many functions in the codes for adjusting, for example, the quadrupole gradients so as to obtain $R_{12} = 0$ & $R_{34} = 0$. It takes about a week to learn the functions of a code, and a few months to learn all the tricks.

In the following picture, we present a spectrometer and the associated beam envelop simulation using the "transportgrafic" code. The dispersion coefficient is presented as well:



The 1st order beam optics simulation of a spectrometer is realized with an optical code, by computing the product of the matrix of each section:

$$R_{\text{spectro}} = R_{\text{driftN}} \dots R_{\text{dipole2}} \dots R_{\text{dipole1}} \cdot R_{\text{drift3}} \cdot R_{\text{quad2}} \cdot R_{\text{drift2}} \cdot R_{\text{quad1}} \cdot R_{\text{drift1}}$$

The matrix R for each kind of electromagnets is well known. The matrix coefficients can depend on parameters such as focal lengths, field strengths, deviation angle ϕ for bending magnets.

The beam transport is simulated in a code step by step: $s_1 \rightarrow s_2 \rightarrow \dots \rightarrow s_N$

We present below the transport matrices for a quadrupole, a free space (called drift), and for a magnetic dipole:

<p><u>Matrix of a quadrupole (x focusing)</u> . where L is its length and $k=G/B\rho_{ref}$ with $G = dB_y / dx$</p>	<p><u>Matrix of a drift length L:</u> γ is the relativistic factor for the reference trajectory</p>	<p><u>Matrix of a dipole magnet with length L & deviation ϕ</u> $L=\phi R$ and $R_{16} = 1 - \cos(kL)$, with $k_x = 1/R$</p>
$R = \begin{bmatrix} \cos\sqrt{k}L & \frac{\sin\sqrt{k}L}{\sqrt{k}} & 0 & 0 & 0 & 0 \\ -\sqrt{k}\sin\sqrt{k}L & \cos\sqrt{k}L & 0 & 0 & 0 & 0 \\ 0 & 0 & \cosh\sqrt{k}L & \frac{\sinh\sqrt{k}L}{\sqrt{k}} & 0 & 0 \\ 0 & 0 & \sqrt{k}\sinh\sqrt{k}L & \cosh\sqrt{k}L & 0 & 0 \\ 0 & 0 & 0 & 0 & 1 & \frac{L}{\gamma^2} \\ 0 & 0 & 0 & 0 & 0 & 1 \end{bmatrix}$ <p><i>horizontal focusing part</i></p> <p><i>Vertical defocusing part</i></p> <p>See APPENDIX 3</p>	$R = \begin{bmatrix} 1 & L & 0 & 0 & 0 & 0 \\ 0 & 1 & 0 & 0 & 0 & 0 \\ 0 & 0 & 1 & L & 0 & 0 \\ 0 & 0 & 0 & 1 & 0 & 0 \\ 0 & 0 & 0 & 0 & 1 & L/\gamma^2 \\ 0 & 0 & 0 & 0 & 0 & 1 \end{bmatrix}$ <p>See exercise A: drifts are not focusing since $R_{21}=0$: the angle x' is not changed for any ion...</p>	$R = \begin{bmatrix} \cos k_x L & \frac{\sin k_x L}{k_x} & 0 & 0 & 0 & R_{16} \\ -k_x \sin k_x L & \cos k_x L & 0 & 0 & 0 & R_{26} \\ 0 & 0 & 1 & 0 & 0 & 0 \\ 0 & 0 & 0 & 1 & 0 & 0 \\ -R_{16} & -R_{26} & 0 & 0 & 1 & R_{56} \\ 0 & 0 & 0 & 0 & 0 & 1 \end{bmatrix}$ <p><i>dispersive part</i></p>

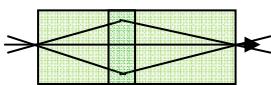
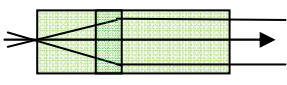
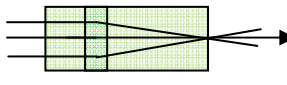
The derivation of the matrices requires a specific lecture on beam optics. It relies on the first order Taylor expansion of the equation of motion in a given analytical field ($B_y=G.x$ for a quad; $B_y=0$ for a drift or $B_y=B_0$ for a dipole), a first approach is presented in the appendix 3.

2.3.8 Designing a new spectrometer

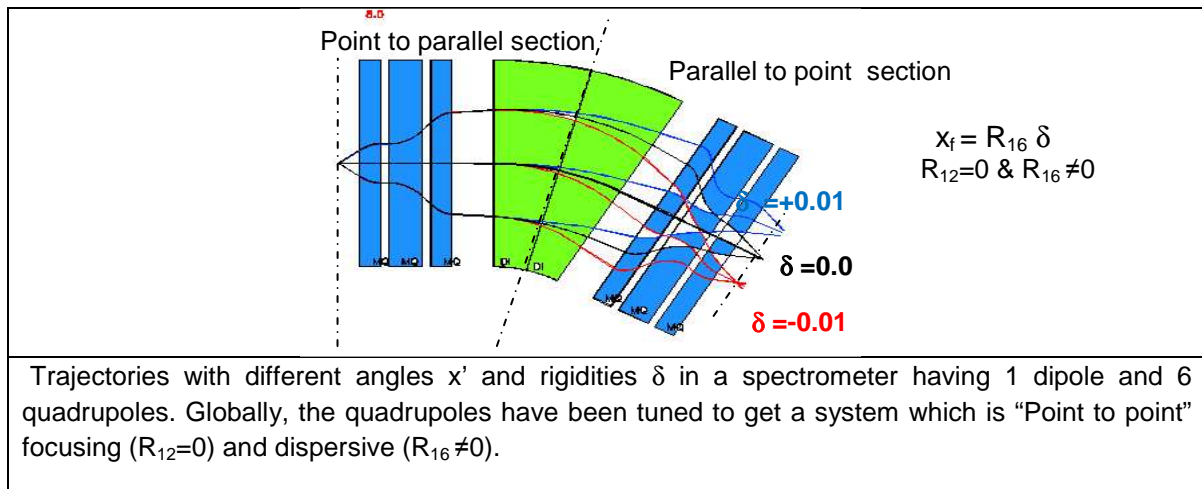
The design of a new spectrometer starts with the first order study (beam envelop and dispersion R_{16}). The different steps to study a new spectrometer are described below:

Step 1) Define the beam of interest after the target (spot size on target, angular distribution, energy dispersion, maximum rigidity $B\rho_{max}$)

Step 2) Adjust the quadrupole sequence (number, length and gradient) to transport the beam with the desired optical properties:

<p>“Point to point” focus</p>  <p>$R_{12}=0$: The final position does not depend on initial angle.</p>	<p>“Point to parallel” focus</p>  <p>$R_{22}=0$: The final angle does not depend on initial angle.</p>	<p>“Parallel to point” focus</p>  <p>$R_{11}=0$: The final position does not depend on initial position.</p>
<p>The different focusing conditions and the corresponding matrix coefficient for an optical system.</p>		

Step 3) Check the dispersion R_{16} and compute the resolution at the final focal point.



Step 4) High order study: few trajectories are computed using realistic magnetic field maps and the Newton-Lorentz equation. The final coordinates are compared with the first order approximation. The goal is to define if the matrix approximation is good enough: this phase is called “optical aberration study”.

When the 1st order approximation is not satisfactory, two cases can be identified:

Case 1) Beam optics simulations have to take into account 2nd order effects, 3rd order....

Case 2) Magnetic multipoles (mainly sextupoles) can be inserted in the spectrometer in order to correct some non-linear effects.

3. SPECTROMETERS AROUND THE COULOMB BARRIER

3.1 Experimental difficulties (low efficiency, charge state pollution)

Reactions around the Coulomb barrier induce phenomena of great diversity (nucleon transfer, elastic scattering, fusion-evaporation, inelastic scattering, fission,...).

The reaction kinematics are so different that the technical methods to optimize the efficiency, the selectivity and the identification are, as well, different. It therefore leads to a wide variety of separators and spectrometers.

Understanding these spectrometers rely mainly on the understanding of the experimental difficulties encountered in each type of reaction.

Problem A: Large emission angle of reaction products and low transmission

The solid angle in fission or multi-nucleon transfer reactions, i.e. the cone emission of reaction products, can be very large (1 steradian), while separators often have a small acceptance, around 10 mstrd, and their efficiency is often very limited (low transmission). However, in these reactions, the emission at a large solid angle of products of interest leaves the possibility of rotating the spectrometer around the target reaction in order to avoid beam scattered particles. This technique can often improve the selectivity of the spectrometer.

Problem B: Charge state distribution

At high energy (500 MeV/A) any ion leaving the target is fully stripped and the charge state corresponds to the atomic number ($Q=Z$). At lower energy, typically a few MeV/A, the primary beam and reaction products are not fully stripped. The distribution of the number of remaining electrons is generally large, since atomic collisions in a target generate numerous electron capture and stripping reactions.

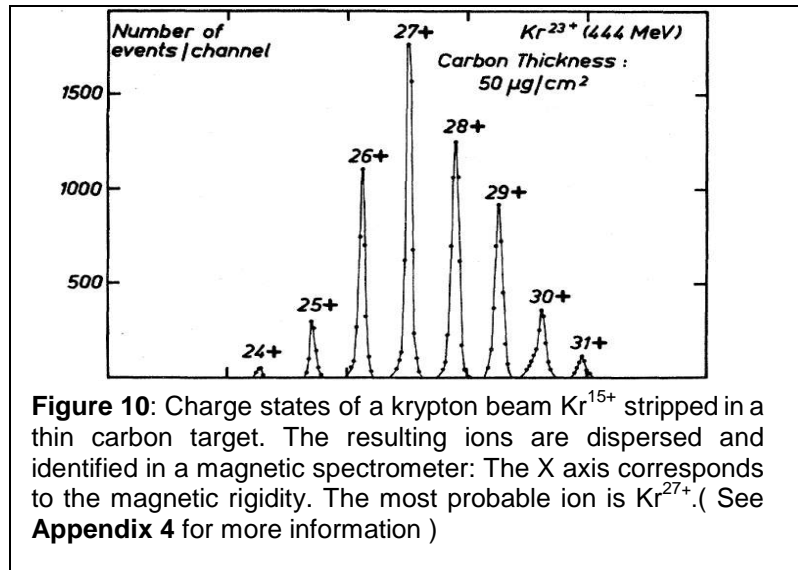
For example, a nucleus with mass ~ 100 , formed by fusion-evaporation, usually has 4 or 5 states charges for an average charge state $\langle q_0 \rangle \sim 25+$. Furthermore, the velocity dispersion is of the order of several %.

Generally the charge states distribution created in a target and transported in a conventional magnetic separator generates two difficulties:

- All the different charge states of the interesting nuclei are not transported to the focal plane ($B\rho$ acceptance). This results in a reduction of the spectrometer transmission:

$$\frac{\Delta B\rho}{B\rho} = \frac{\Delta q}{\langle q_0 \rangle} + \frac{\Delta v}{\langle v_0 \rangle} \gg 10\% > B\rho \text{ acceptance}$$

- The primary beam emerges from the target with so many charge states (with different $B\rho$), that the focal plane is polluted over a large range in $B\rho$, which often prevents to measure very rare events.



Problem C: Contaminants (beam charge states and other kinds)

The nuclei of interest are often polluted by particles whose intensity is often too large to be accepted by the detection system.

These particles to be eliminated (bad events) are of several types:



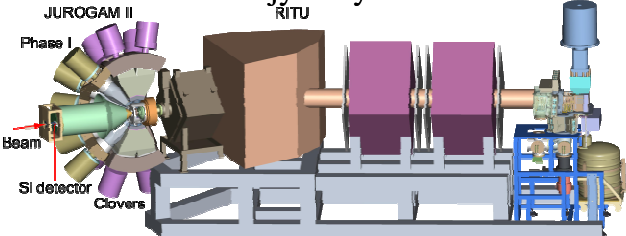
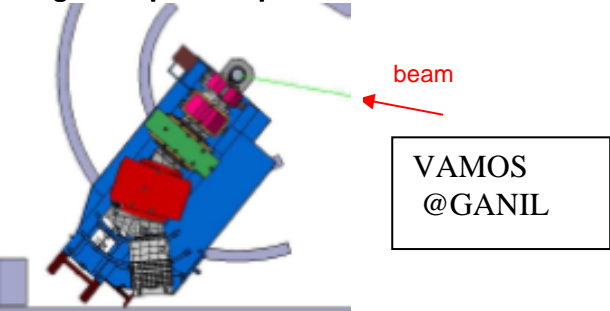
- Charge states of the primary ion beam (slowed down in the target by multiple interactions with the target atoms).
- Beam particles, elastically scattered by the Coulomb potential of target nuclei.
- Target ions, elastically scattered by the beam particles (recoil of target nuclei).
- Particles produced by nuclear reactions with a large cross section (fission, fusion, nucleon transfer, ...).

Many problems, many solutions:

The technical problem of the contaminants, charge states and low transmission, can be partially overcome for each reaction type. This results in different spectrometers and separator technology well adapted for each reaction kinematics.

Whatever the solution proposed, the essential quality for the different devices is the rejection (elimination) of the primary beam particles.

In the following table we present different separator technologies for each physics domain:

Reaction examples	Difficulties	spectrometers and technologies
<p>Transfer reaction:</p> $^{136}\text{Xe} (7.5\text{MeV/A}) + ^{48}\text{Ca} \Rightarrow ^{52}\text{Ca}$ <p>- Large angular distribution of the transfer products</p> <p>- Product are emitted at the grazing angle ($\sim 45^\circ$)</p>	<p>- Low angular transmission</p> <p>- Rejection of primary beam difficult at 0°</p> <p>Few products a zero degree (spectrometer should be rotated)</p>	<p>- Large acceptance spectrometer ex: PRISMA, VAMOS, MAGNEX</p> 
<p>Fusion-evaporation:</p> $^{58}\text{Ni} (4.5\text{MeV/A}) + ^{64}\text{Ni} \Rightarrow ^{120}\text{Ba} + 2n$ <p>Large velocity difference between the beam particles & the reaction products</p>	<p>- Z identification difficult ($E < 1\text{MeV/A}$)</p> <p>- Rejection of primary beam charge states difficult (same B_p as the products)</p>	<p>- M/q spectrometer using Electric fields ex: RMS Jaeri, RMS, EMMA</p> 
<p>Superheavy synthesis:</p> <p>- Charge states</p> <p>- Primary beam pollution</p> $^{48}\text{Ca}(4.5\text{MeV/A}) + ^{206}\text{Pb} \Rightarrow ^{252}\text{No} + 2n$ <p>\Rightarrow Large velocity difference between the beam particles & the reaction products</p>	<p>- Very rare events</p> <p>- Direct identification not possible ($E \sim 0.1\text{MeV/A}$)</p> <p>- Very intense primary beam ($P > 1\text{ kW}$)</p> <p>The rejection of primary beam charge states is difficult (same B_p as the reaction products)</p>	<p>- gas filled separator (ex: RITU, DBGS, GARIS, TASCA)</p> <p>Ritu@jyvaskyla RITU</p>  <p>- Electrostatic Separator (ex: VASSILISSA)</p> <p>- Velocity Filter with B and E fields: Wien filter (E and B crossed) Or Velocity Filter with E+B (SHIP)</p> <p>Associated techniques:</p> <ul style="list-style-type: none"> - Rotating target (high beam power) - Identification with decays after implantation (α, \dots)
<p>Fission:</p> $^{238}\text{U}(6\text{MeV/A}) + ^{12}\text{C} \Rightarrow ^{130}\text{Sn}$ <p>Large angular distribution of the fission fragments</p> <p>- Fragments are not emitted at 0° ($\sim 20^\circ$)</p>	<p>- Low angular transmission</p> <p>Few products at 0° (the spectrometer should be rotated)</p>	<p>- Large acceptance spectrometer</p>  <p>VAMOS @GANIL</p> <p>Vamos is mounted on a rotating platform</p>

3.2 Large acceptance spectrometers

A new class of magnetic spectrometers emerged in the early 2000s, pushing the angular acceptance to values close to 100 mstrd. These spectrometers have been designed to maximize the transmission efficiency. Nonlinearities in optics are such that they require a high performance detection system and numerical reconstructions of the paths for the ion for their identification.

The 1st order approximation allows a quick simulation of the trajectories in the spectrometer. However, it is just an approximation. The non-linear dependencies, called aberrations, are inducing several effects:

- 1) The focal plane is not perpendicular to the beam axis.
- 2) The large angle particles are over-focused by the quadrupoles
- 3) The particles with a Bp different from the reference ion are not properly focused

Such effects always exist but are often too small to be observed in small acceptance spectrometers.

In large acceptance spectrometers, non-linear effects have a large magnitude and the Bp measurement relies on a complex equation involving non linear dependencies in position and angle because of the aberrations.

3.2.1 Non-linearity (optical aberrations)

The approximation that the final coordinates of the particles are linear combinations of the initial coordinates is not valid when we are considering a particle whose coordinates are far from the reference particle (large angle θ , $\phi > 30\text{mrad}$, or large Bp deviation: $\delta > 1\%$)...

For a spectrometer with a very large acceptance, a precise simulation has to be performed using the magnetic field maps of the optical elements (quadrupoles, dipoles...).

The exact dynamics of the ions in the spectrometer can be written as a Taylor expansion using the initial coordinate $Z_0 = (x_0, x_0', y_0, y_0', l_0, \delta_0)$:

$$Z_{f_i} = \sum_{j=1, \dots, 6} (Z_i | Z_j) Z_{0_j} + \sum_{j,k=1, \dots, 6} (Z_i | Z_j Z_k) Z_{0_j} Z_{0_k} + \sum_{j,k,l=1, \dots, 6} (Z_i | Z_j Z_k Z_l) Z_{0_j} Z_{0_k} Z_{0_l} + \dots$$

$$Z_f = 1^{\text{st}} \text{ order terms} + 2^{\text{nd}} \text{ order} + 3^{\text{eme}} \text{ order} + \dots$$

The coefficients $(Z_i | Z_j) = R_{ij}$, $(Z_i | Z_j Z_k)$ et $(Z_i | Z_j Z_k Z_l)$ are the coefficients of the 1st, 2nd, et 3rd order of the transfer map of the optical system. The non-linearity makes difficult the reconstruction of the quantity of interest (especially the Bp).

Starting from $X_f = R_{16} \delta \Rightarrow$ the inversion gives $\delta = X_f / R_{16}$ or $B_p = B_{p0} (1 + X_f / R_{16})$


This is a linear equation in x_f

With the non-linearity, we have

$$X_f = R_{16} \delta + (x | x x) x_0 x_0 + (x | x' x) x_0' x_0 + (x | x' x') x_0' x_0' + \dots + (x | \delta \delta) \delta \delta + (x | x x x) x_0 x_0$$

The coefficients $(x | x^n x^m \delta^k)$ are called the aberration coefficients, they correspond to the non linear generalization of the transport matrix coefficient R_{ij} .

The inversion, from $X_f=f(\delta)$ to $\delta=f^{-1}(X_f, \dots)$, is not trivial, even if you know the aberration coefficients ($x|x^n x^m \delta^k$): since the initial parameter (x_0, x_0', \dots) are not measured:

$$\delta = X_f/R_{16} - (x/x x') x_0 x_0 + \dots + \dots \quad \text{Initial coordinates (not measured) ???}$$


Using a trajectory simulation, We generally try to adjust a form like

$$\delta = F(x_f, x_f', y_f, y_f', a, b, c, d, \dots)$$

Or in a more obvious form:

$$B\rho = B\rho_0 (1 + x_f/R_{16} + a x_f^2 + b x_f'^2 + c x_f^3 + d x_f'^3 + \dots)$$

Hence, a possible technique is to fit the unknown coefficients, (a,b,c,d,...) in the last expression, with a trajectory simulation using realistic magnetic field maps.

3.2.2 Identification in a magnetic spectrometer

The identification method for a single ion (A, Z, energy, q) with a magnetic spectrometer depends on several measurements. The quantities (A, Z, E, q) are not directly accessible and must be computed using different measured parameters. There are 4 independent quantities to reconstruct, so at least four independent measurements are required:

Method of reconstruction:

- 1) Measurement of the position x_f after the spectrometer (at the focal plane)
- 2) Measurement of the Time of Flight (ToF)
- 3) Measurement of the energy loss ΔE in a thin detector (silicon or ionization chamber)
- 4) Measurement of the residual energy E_r .

Then we can compute $B\rho = B\rho_0 (1 + x_f/R_{16} + \dots + \dots)$

M/q	$M/q = B\rho_0/v = B\rho * T \text{ fligth} / L_0$
Z	$Z \sim k \Delta E \dots$
A	$A = (E_r + \Delta E) / (\gamma v^2)$
q	$q = A / [M/q]$

The properties of the spectrometer have to be known:

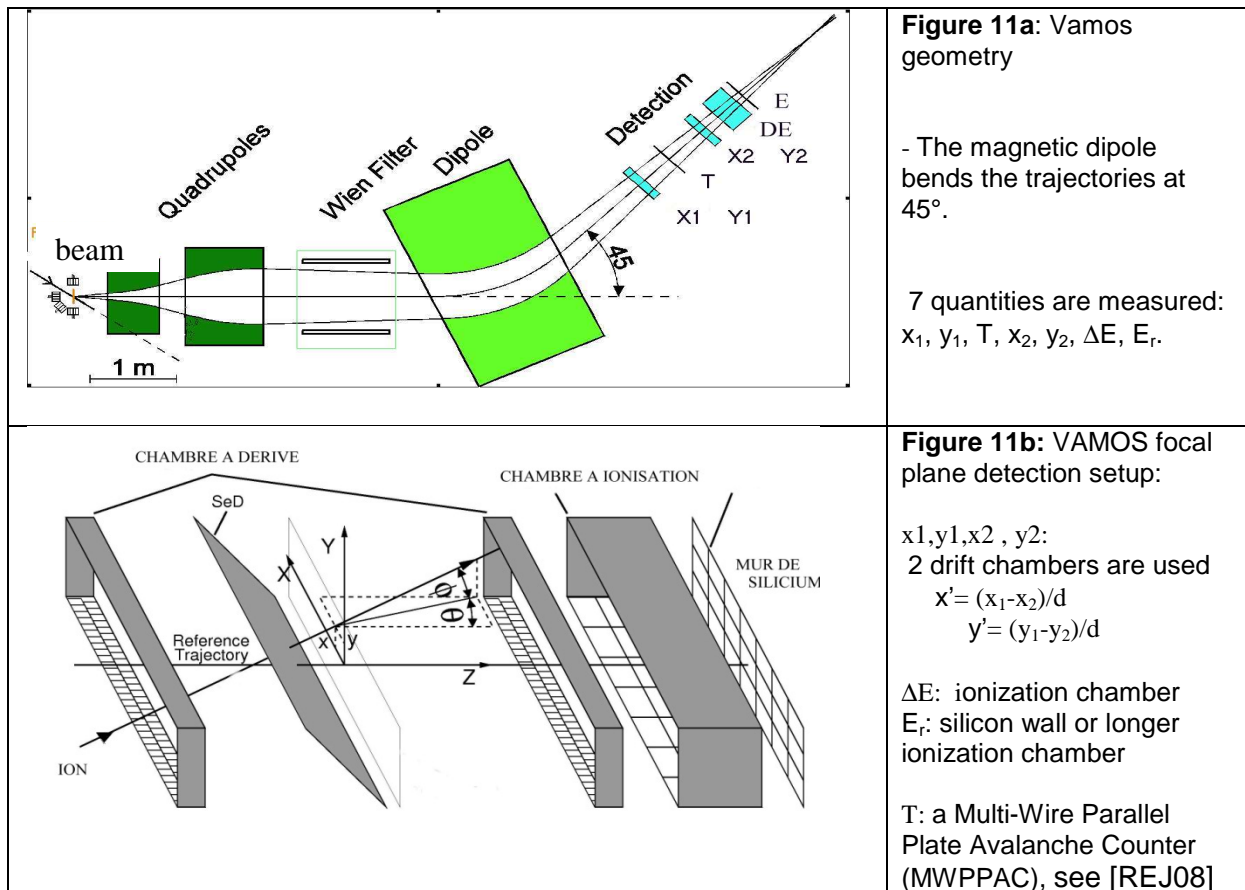
Flight length L, dispersion R_{16} , curvature of the dipole R_m (curvature of the reference trajectory) and the **magnetic field B** of the dipole ($B\rho_0 = B R_m$)

3.2.3 The VAMOS spectrometer at GANIL

The VAMOS spectrometer (VARIABLE MOde Spectrometer) [SAV99] has been designed for the use of radioactive beams produced by the ISOL method and accelerated by the cyclotron CIME at GANIL. It is also used with stable beams for transfer and fission-induced reactions.

The VAMOS geometry consists in a quadrupole doublet, a velocity filter (not often used) and a dipole magnet.

VAMOS is a large solid angle ray-tracing spectrometer employing numerical methods for reconstructing the particle trajectories. Complete identification of reaction products is achieved by a trajectory reconstruction.



Reconstruction method in three steps

For the reconstruction, the quantities of interest ($B\rho, A/Q$) are derived from the measurements performed at the focal plane $Z_f(x_f, x'_f, y_f, y'_f)$. The following method is used:

Step a) a trajectory simulation of thousands of particles is realized ($Z_0 \Rightarrow Z_f$) with a transport code using the magnetic field maps of the quadrupoles and dipole. The Newton-Lorentz equation is integrated to compute the trajectory of different ions with a multi-particle tracking code (see APPENDIX 2).

Step b) Then, the initial coordinates can be represented as polynomials of the final coordinates with many coefficients ($a_1, b_1, c_1, d_1, \dots$). The coefficients can be adjusted (fitting procedure) using the thousands simulated trajectories. 4 polynomials are obtained:

$$B\rho = f_1(x_f, x'_f, y_f, y'_f, a_1, b_1, c_1, d_1, \dots) \quad \text{polynomial to the 7th order in } (x_f, x'_f, y_f, y'_f)$$

$$L_{flight} = f_2(x_f, x'_f, y_f, y'_f, a_2, b_2, c_2, d_2, \dots)$$

The polynomial coefficients ($a_1, b_1, c_1, d_1, \dots$) of the inverse transfer map are fitted, using the numerical simulation of the ions in the spectrometer. This fit is realized with a χ^2 minimization for f_1 and f_2 :

$$\chi^2 = \sum_{i=1, N_{traj}} (B\rho_i - f_1(x_f, x'_f, y_f, y'_f, a_1, b_1, c_1, \dots))^2 \quad \frac{\partial \chi^2}{\partial a_1} = 0, \quad \frac{\partial \chi^2}{\partial b_1} = 0, \dots$$

The χ^2 minimization is performed by a SVD ("singular value decomposition") algorithm. This fit is a very important and delicate work, since some of the coefficients are not well determined: these coefficients have to be constrained to zero during the fit.

Step c) During the experiment, (x_f, x'_f, y_f, y'_f) are measured and $B\rho$ is computed using the aberration coefficients a_1, b_1, c_1, \dots

$$B\rho = f_1(x_f, x'_f, y_f, y'_f, a_1, b_1, c_1, d_1, \dots)$$

$$= B\rho_0 (1 + x_f/R_{16} + a_1 x_f^2 + b_1 x_f'^2 + c_1 x_f^3 + d_1 x_f'^3 + \dots)$$

For the velocity, the time of flight is measured between the target and the focal plane:

$$v = \text{Time of flight} / L_{\text{flight}} = \text{Time of flight} / f_2(x_f, x'_f, y_f, y'_f, a_2, b_2, c_2, d_2, \dots)$$

The approximate mass number M comes from the energy measurement:

$$M \sim 2 \cdot \text{focal plane energy} / v^2$$

And the particle identification comes from the couple $(v, B\rho)$: $A/Q = B\rho / \gamma \cdot v$

While the charge state is given by: $Q = ([A/Q] / [M])^{-1}$

For a good reconstruction of the magnetic rigidity in VAMOS, more than 500 coefficients (a, b, c, \dots) are needed, using corrections up to x_f^7 (seventh order).

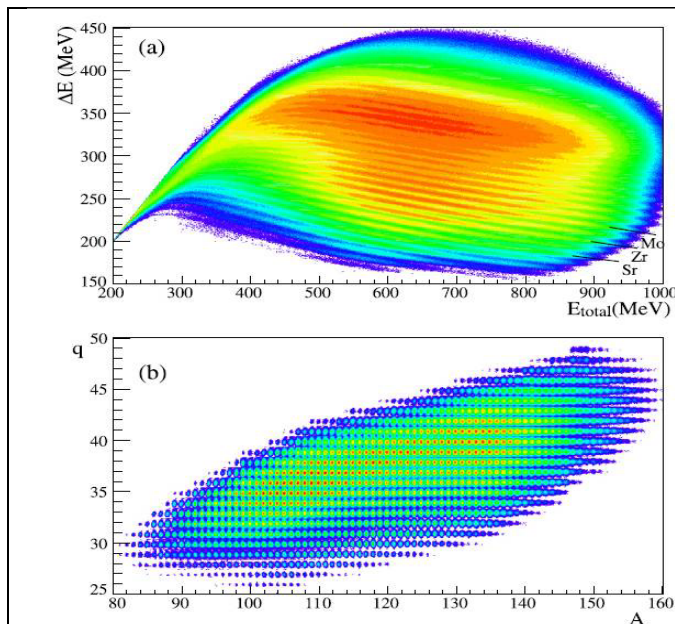


Figure 12: Identification of fission fragments in VAMOS in the $^{12}\text{C}(^{238}\text{U}, \text{ff})$ reaction.

(a) $(E, \Delta E)$ plot: line structures correspond to different Z values ($Z=34$ to $Z=50$)

(b) (A, Q) plot: obtain after reconstruction

About 2400 ions species have been identified in one single fission experiment:

5 charge states \times 6 Z values for each mass... \times 80 Masses

[M.Rejmund, private communication]



Figure 13:

Top view of VAMOS.

The real spectrometer has been carefully simulated to find the relationship between the final coordinate and the $B\rho$:

$$B\rho = f_1(x_f, x'_f, y_f, y'_f, a_1, b_1, c_1, d_1, \dots)$$

3.2.4 Large acceptance spectrometers in the world

Spectrometer	VAMOS GANIL (Caen)	PRISMA LNL (Legnaro)	MAGNEX LNS (Catania)
geometry	$q_v q_h B$	$q_v B$	$q_v B$
rotation	$0^\circ - 60^\circ$	$0^\circ - 50^\circ$	$0^\circ - 50^\circ$
Bpmax	1.7 T.m	1.2 T.m	1.8 T.m
Angular Acceptance	70 mstrd	80 mstrd	55 mstrd
Bp Acceptance	$\pm 25\%$	$\pm 10\%$	$\pm 10\%$
Length	8m	6.5m	7m
Angle	$(0^\circ - 60^\circ) 45^\circ$	45°	55°
Dipôle gap	200mm	200mm	200mm
dispersion	$\sim 1.8 \text{ cm}/\%$	$2 \text{ cm}/\%$	$1.5 \text{ cm}/\%$
Resolution Bp	1/1000	1/2000	1/2000
Resolution Tof	1/200	1/500	1/200
Mass Resolution	1/170	1/500	1/200
Resolution Z	1/50	1/60	
Domain	- Transfer with RIB // reaction induced fission	- Transfer	- Transfer

* B= magnetic dipole // q_h =quadrupole focusing in horizontal // q_v = vertical focusing

In the case of PRISMA and MAGNEX, a single quadrupole is used to focus the beam in the vertical plane, while the magnetic dipole with specific edges can focus slightly in x (see APPENDIX).

Note that certain performances depend not only on the spectrometer but on the optical quality of the primary beam. For example, the Bp resolution also depends on the size Δx_0 in the horizontal plane of the primary beam on the target (see "resolution of a spectrometer," Chapter 2).

3.3 The so-called « Mass » Spectrometer (M/q)

3.3.1 Magnetic versus M/q spectrometer principle

A magnetic spectrometer (which includes bending magnets) disperses laterally the particles as a function of P/Q, the so called magnetic rigidity Bp. The final position X_f is not only a function of the Mass and Charge but has a velocity dependence:

$$Bp = \gamma Mv/Q = Bp_0 (1 + x_f/R_{16})$$

One should know the velocity v to compute M/Q . Hence for a magnetic spectrometer, the dynamical parameter to be considered for the optics is δ :

$$\delta = \frac{p/Q - p_0/Q_0}{p_0/Q_0}$$

The coordinate of particles will include simply δ , which is the unique dynamical parameter.

$$\mathbf{Z}^0 = (Z_1^0, Z_2^0, Z_3^0, Z_4^0, Z_5^0, Z_6^0) = (x, x', y, y', l, \delta)$$

In nuclear physics, the “beams” of reaction products have generally a very large velocity dispersion: The bending magnets will not permit to separate laterally the ions having different masses because of the velocity dependence.

A combination of two devices, an electrostatic deflector and a bending magnet, can lead to a system that disperses laterally the ion as function of their “mass over charge ratio” ($m=M/Q$), but irrespective to their velocity. This is a “mass over charge” spectrometer (improperly called mass spectrometer).

3.3.2 Beam optics with electrostatic and magnetic deflection

In such a spectrometer, one needs to know two parameters ($B\rho, M/Q$) or ($B\rho, E\rho$) at the same time to describe the trajectory in magnetic and electric field. Since the electrostatic deflector disperses laterally the particles as a function of Pv/Q , the knowledge of the parameter P/Q is not sufficient to describe the trajectories.

In order to describe the ions trajectories in a mass spectrometer, we propose to add the parameter M/Q . So, we need a seventh coordinate, instead of 6 coordinates as in a magnetic beam line: the new parameter is the mass over charge ratio deviation δm :

$$\delta_m = \frac{M/Q - M_0/Q_0}{M_0/Q_0}$$

So, the coordinate vector of particles will include δ and δ_m :

$$\mathbf{Z}^0 = (Z_1^0, Z_2^0, Z_3^0, Z_4^0, Z_5^0, Z_6^0, Z_7^0) = (x, x', y, y', l, \delta, \delta_m)$$

$$\bar{z} = \begin{pmatrix} z1 \\ z2 \\ z3 \\ z4 \\ z5 \\ z6 \\ z7 \end{pmatrix} = \begin{pmatrix} x \\ x' = \frac{dx}{ds} \\ y \\ y' = \frac{dy}{ds} \\ l = v_0(T - T_0) \\ \delta = \frac{p/Q - p_0/Q_0}{p_0/Q_0} \\ \delta_m = \frac{M/Q - M_0/Q_0}{M_0/Q_0} \end{pmatrix} = \begin{pmatrix} \text{horizontal displacement} \\ \text{horizontal "angle"} \\ \text{vertical displacement} \\ \text{vertical angle} \\ \text{longitudinal difference} \\ \text{B\rho deviation} \\ \text{"mass (M/Q)" deviation} \end{pmatrix}$$

In most of the beam lines, we can consider particle having a fixed mass M_0 and a fixed charged state Q_0 :

But, in a mass spectrometer, a seventh parameter become useful $\Leftrightarrow \delta_m$:

A new transfer matrix coefficient appears, the summations run up to 7 instead of 6:

$$\mathbf{Z}_i^F = \sum_{j=1..7} R_{ij} Z_j^0 + \sum_{j=1..7} \sum_{k=1..7} T_{ijk} Z_j^0 Z_l^0 + \dots$$

Hence, a spectrometer including electric and magnetic field matrices can be written as

$$\begin{bmatrix} x \\ x \\ y \\ y \\ l \\ \delta \\ \delta m \end{bmatrix}_F = \begin{bmatrix} R_{11} & 0 & 0 & 0 & 0 & R_{16} & R_{17} \\ R_{21} & R_{22} & 0 & 0 & 0 & R_{27} & R_{27} \\ 0 & 0 & R_{33} & 0 & 0 & 0 & 0 \\ 0 & 0 & R_{43} & R_{44} & 0 & 0 & 0 \\ R_{51} & R_{52} & 0 & 0 & L/\gamma^2 & 0 & 0 \\ 0 & 0 & 0 & 0 & 0 & 1 & 0 \\ 0 & 0 & 0 & 0 & 0 & 0 & 1 \end{bmatrix} \cdot \begin{bmatrix} x \\ x \\ y \\ y \\ l \\ \delta \\ \delta m \end{bmatrix}_0$$

$$l = v_0(t - t_0)$$

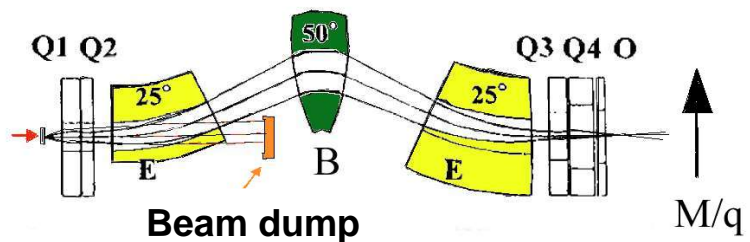
$$\delta = \frac{p/Q - p_0/Q_0}{p_0/Q_0}$$

$$\delta m = \frac{M/Q - M_0/Q_0}{M_0/Q_0}$$

If the electrostatic deflector(s) balance the magnetic dipole(s), it is possible to get $R_{16}=R_{26}=0$ (achromatic) while $R_{17} \neq 0$ (M/Q dispersion). Such a combination is called "Recoil Mass Spectrometer" (RMS):

The RMS spectrometer has been used in numerous laboratories [COR83, IKE96]. It permits to select ions as function of the parameter M/q . Since the electrostatic deflectors are very limited in bending power for high energy particles, these devices are limited to low energy nuclear physics [1-3MeV/A].

Figure 14: Here the Recoil Mass Spectrometer of JAERI (Japan). It is composed of 2 electrostatic deflectors (25°), and a magnetic dipole (50°). An octupole corrects part of the non linearities (aberrations).



Generally the primary beam is stopped on a beam dump after the first electrostatic deflector.

The RMS spectrometer principle possesses two main advantages:

A good rejection of the primary beam:

In fusion reactions the difference in velocity between the primary beam and evaporation products is usually very large. An electrostatic device separates the ions as a function of $E_p = \gamma Mv^2/q$, which is more efficient than the magnetic device which works with $B_p = \gamma Mv/q$.

A direct measurement of the M/q ratio

The cancellation of the R_{16} coefficient with the E+B+E symmetric structure permits to obtain a direct relationship between position and Mass over charge ratio, which eases the identification:

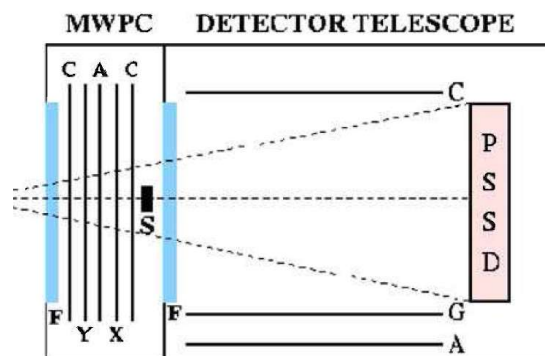
$$M/Q = M_0/Q_0 (1 + x_f/R_{17}), \text{ Where } R_{17} = \partial x_f / \partial M/q$$

3.3.3 Ion identification in a mass spectrometer

The quantities (A, Z, E, q) are not directly available, they are derived from different measurements: The final position x_{focal} of the ions and possibly their time of flight and energies are needed. We present in figure 15 a typical detection system for a spectrometer:

Figure 15: Focal plane detection of HIRA, New Dehli [JIN04]. 3 detectors are used:

- 1) **MWPC** (Multi-Wire Proportional Counter): positions X1 Y1 and time T1. 2 plastic foils (C) generate secondary electrons measured by a wires mesh (A). A voltage of about 800 V is applied between A and C.
- 2) **ΔE telescope:** ionization chamber (isobutane). G = Frish Grid; A = anode; C = cathode.
- 3) **PSSD:** (Position Sensitive Silicon Detector) :positions X2 and Y2, and Energy E. The resolution obtained in x,y is $R=0.9$ mm



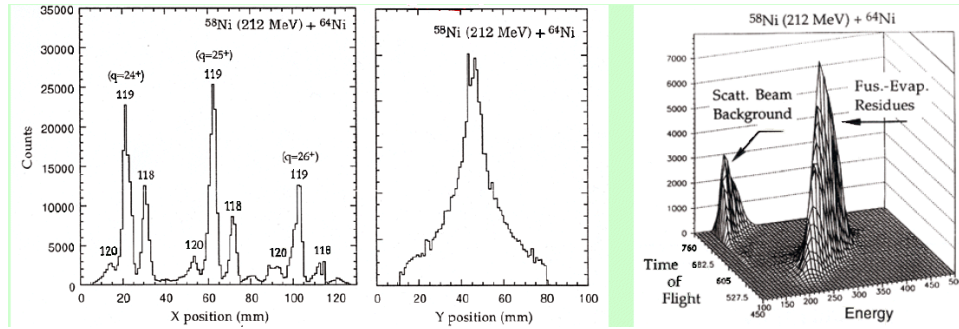


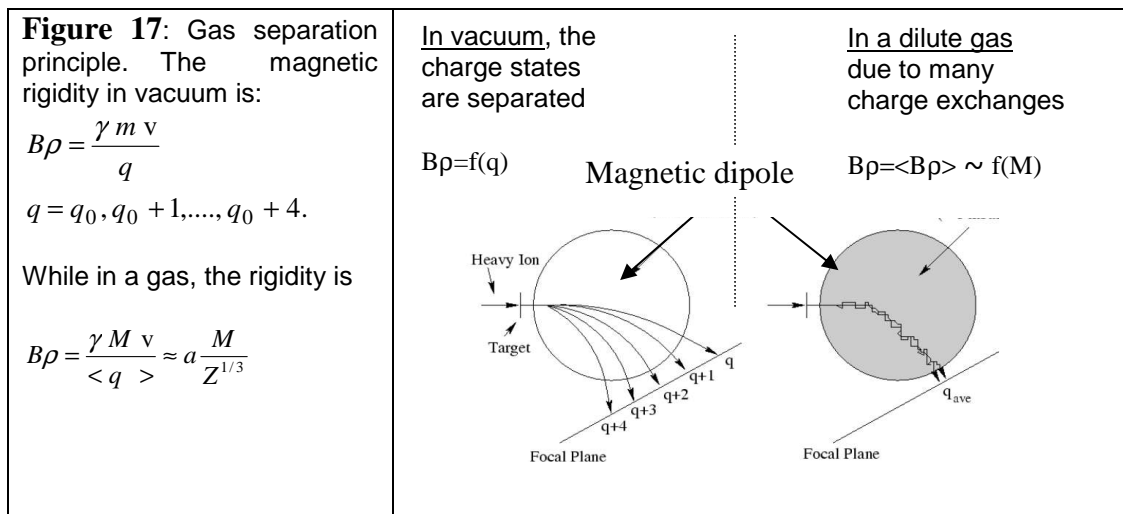
Figure 16: The ions produced in the fusion-evaporation reaction $^{58}\text{Ni} + ^{64}\text{Ni}$ are measured in the focal plane of a RMS-type spectrometer. The left part shows the horizontal position of the different peaks corresponding to the ratio $M/q = 118/24, 119/25 \dots$ in the focal plane of the spectrometer. The tails of the distribution (right picture) correspond to scattered primary beam particles (central part) reaching the detection setup. It is possible to eliminate them during the analysis by applying a ToF versus E condition.

3.3 Gas filled separators

Historically this principle was used for the study of fission fragments (Oak Ridge then Jülich). In recent years, the principle is applied mainly to the fusion reaction studies including superheavy synthesis. In 2008, 5 gas separators were in operation in the world. This principle of separation overcomes some limitations of conventional magnetic separators in terms of efficiency and selectivity.

3.3.1 Principle of selection in a gas [LEI99, PAU89]

When an ion moves in a diluted gas, the charge state ($q = Z - N_{\text{bound electrons}}$) fluctuates along its course. Indeed, collisions between the ion and the gas molecules induce electron captures and losses. When collisions are frequent, the trajectory of an ion in a gas filled magnetic dipole is determined by its average charge states $\langle q \rangle$, corresponding to the center of the charge state distribution.



The average charge state $\langle q \rangle$ depends mainly on the ion atomic number (Z) and on its velocity:

$$\langle q \rangle \approx a v Z^{1/3}$$

So in a given gas, the rigidity is in average mainly proportional to the mass M :

$$B\rho = \langle B\rho \rangle = \frac{\gamma M v}{\langle q \rangle} \approx a \frac{M}{Z^{1/3}}$$

In a gas filled spectrometer, the ion $B\rho$ is independent of the velocity and the charge. The selection is therefore a function of M (and Z).

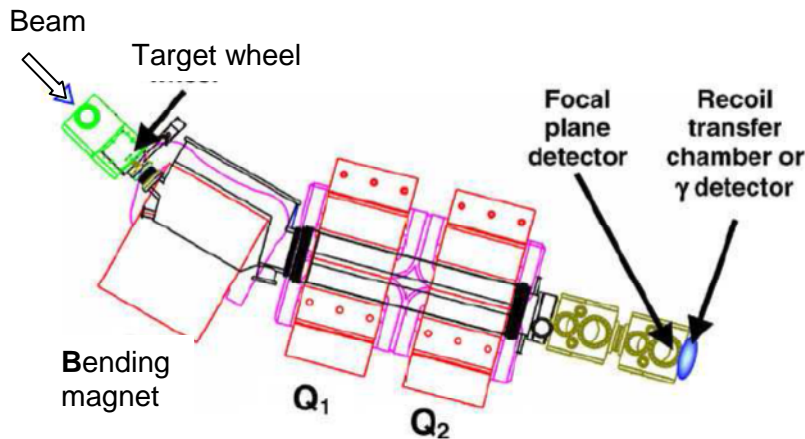


Figure 18: Tasca @GSI

This gas filled separator uses the BQQ geometry. The target is very close to the dipole in order to eliminate the primary beam as soon as possible. This geometry improves the rejection but it reduces the angular acceptance, since the quads are too far from the reaction target.

In fusion-evaporation reactions, in a standard magnetic spectrometer, one gets always some charge states having the right $B\rho$ and arriving on the focal plane detector. In contrast, the gas filled mode allows a perfect elimination of all primary beam particles in fusion reactions since it permits a mass selection (independent to the ion charge state).

3.3.2 The gas used in separators

The helium gas is used in most cases, at a pressure between 0.5 mbar and 1.0 mbar, while the working pressure in the accelerator beam lines is 10^{-6} mbar. Hence, there are 6-7 orders of magnitude of pressure difference between them.

A carbon window can be used between the target and the upstream beam line to isolate the separator from the vacuum of the accelerator. In some cases, a costly differential pumping system can be installed to avoid the carbon window that generates unwanted reactions.

An accurate empirical model to predict the mean charge state $\langle q \rangle$ in He gas is given in [SAR11]:

$$\langle q \rangle_{He_gas}(Z, v_{out}) = 0.00871 \cdot \left(\frac{v_{out}}{v_0} \right)^{1.54} Z^{1.10} + 2.05$$

where $v_0 = 2.188 \times 10^6$ m/s. Z is the projectile atomic number and v_{out} its velocity at the exit of the production target.

The collisions and charge exchanges make the beam optics fuzzy (the ions straggle during their transport), so the beam becomes very large in the focal plane ($\Delta x = 5-10$ cm).

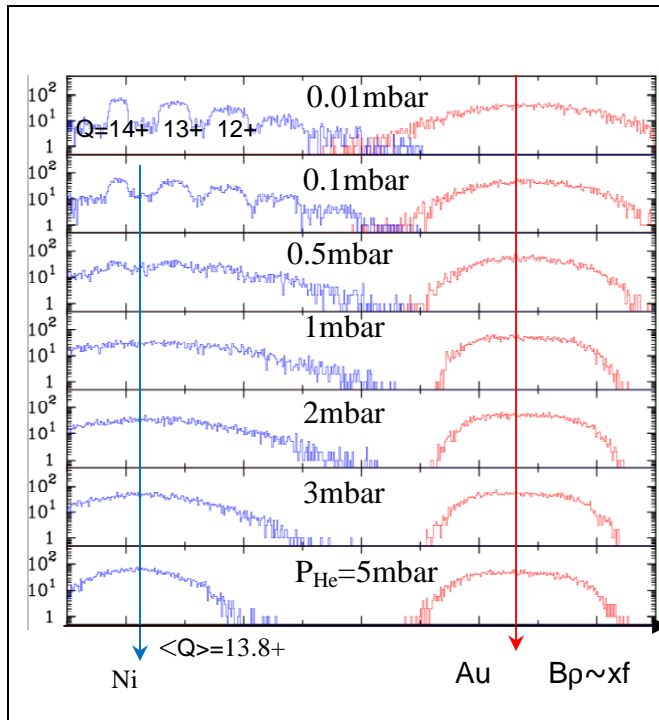


Figure 19a: Simulation code "Trajig"

Separation in He gas of two ions produced in an elastic scattering reaction: $^{64}\text{Ni}(220 \text{ MeV}) + ^{197}\text{Au} @ 60^\circ$

Spectrometer with 3° acceptance and $R_{16} = 2. \text{cm} / \%$.

$^{197}\text{Au} \rightarrow A/Z^{1/3} = 46$ 50% difference in Bp
 $^{64}\text{Ni} \rightarrow A/Z^{1/3} = 21$ $(21-46)/46 = 0.5$

^{64}Ni energy @ $60^\circ = 2.45 \text{ MeV/u}$

^{197}Au energy @ $60^\circ = 0.3 \text{ MeV/u}$

At 0.01 mbar, the peaks correspond to Ni charge states. They are seen at different Bp. At 0.5 mbar, the numerous charge exchanges, reduces the distribution to a single narrower one with mean charge state $\langle Q \rangle$.

*Presentation of Fernando Scarlassara
 [for PRISMA test in a gas filled mode]*

3.3 Transmission and rejection of a gas filled separator

The superheavy synthesis requires to evaluate and to optimize the transmission and the rejection in a gas filled separator.

The evaluation of the transmission is needed for the measurement of the reaction cross-section. It is deduced from the corresponding recoil rate at the focal plane of the separator. For such a purpose, a well known reaction has to be used to evaluate the transmission. However the numerous uncertainties (excitation function, angular distribution, energy distribution, straggling in the target) make difficult to give precise transmission estimates.

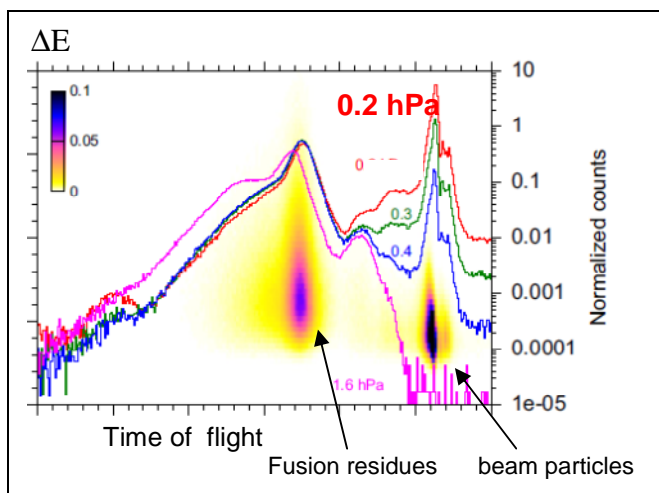


Figure 19b:

$(\Delta E, \text{ToF})$ spectrum for different He gas pressures in the test reaction

$^{40}\text{Ar} (4 \text{ MeV/A}) + ^{150}\text{Sm} \Rightarrow ^{186}\text{Hg} + 4n$

The rate indicated corresponds to contamination (scattering, non equilibrated charge state).

At a pressure higher than 0.4 mbar (=0.4 hPa), the counting rate is acceptable, (see the blue curve). The rejection optimal at $P > 0.6 \text{ mbar}$.

Adapted from [SAR11]

The rejection is generally easy to measure for any reaction kinematic:

$$\text{Rejection} = I_{\text{beam}} / \text{focal detector rate}$$

In fusion reactions with direct kinematics (light beam on heavy target), the primary beam rejection can be very high while in symmetric reactions the rejection is less favorable since the relative Bp deviation between beam and residues is 25% instead of 50-70% in the

very asymmetric cases (for instance Ne beam +Pb target). The reactions in inverse kinematics (for instance, Pb beam on a Ca target) cannot be studied: the proximity in B_p of the fusion residues and the incoming beam prevents the separation in any magnetic separator.

4. SEPARATORS AT HIGH ENERGY

4.1 Reactions at high energy ($1\text{ GeV} > E > 100\text{ MeV}$)

The production and the study of nuclei have some advantages at high energy:

- The incident ions have a large range in materials, so relatively thick reaction targets can be used for improving production rates.
- The reaction products are forward focused leading to a better transmission: For example, the kinematics of the fragmentation of a projectile at energies of the order of $100\text{ MeV} / A$, ensures that a majority of the reaction products leaves the target and is forwardly directed in a cone with $\pm 50\text{ mrad}$. In addition, in this case the energy spread of the fragments is typically of 2-3 percent, which is close to the acceptance of a magnetic separator.
- The ions are generally fully stripped, ($Q=Z$), so the identification is easier.

However, high energy reactions have a major economic drawback: It requires expensive accelerators and large spectrometers using often superconducting magnets adapted for high rigidity beams (BigRips@Riken 77 m, $B\rho^{\text{max}}=7.0\text{ T.m}$. SuperFRS Project @GSI: 120 m, $B\rho^{\text{max}}=20\text{ T.m}$).

4.2 « Fragment separator » for in-flight fragmentation

Fragmentation reactions ($E > 100\text{ MeV} / A$) are known since the 1970's to be very efficient to produce very exotic nuclei. However, the too rich spectrum of the ions has hindered, for a time, the study of exotic species produced by this method.

The main challenge was to invent a new method of purification, allowing the study of the reaction products. In the years 1980-90, the LISE fragment separator, proposed for the first time an efficient selection method with an angular acceptance of $\pm 20\text{ mrad}$. [ANN87]

The principle of the separator is based on 2 sections:

1st Section: $B\rho$ selection ($R_{16} \neq 0$)

2nd section: dispersion compensation, besides the insertion of a wedge-shaped degrader after the first section makes a "Z selection" possible

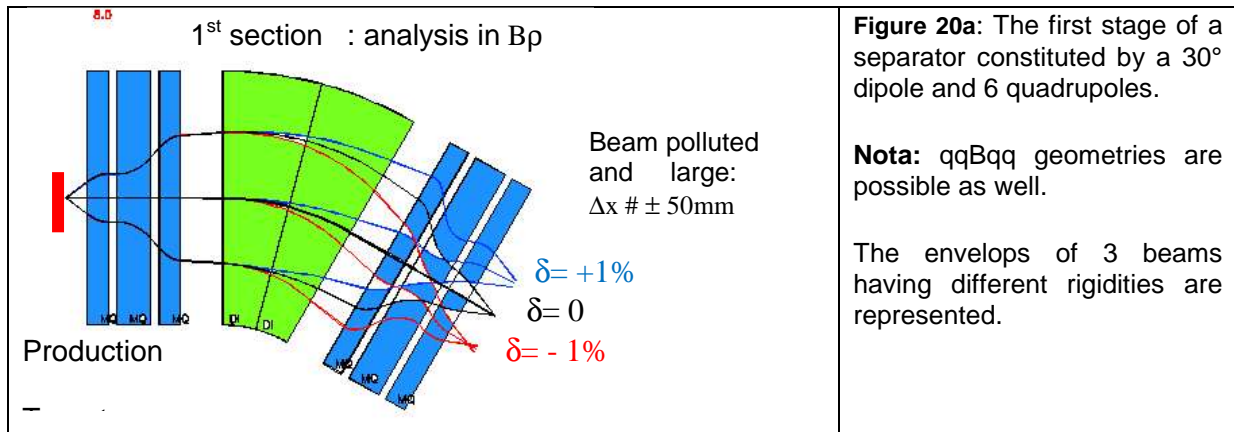
The combined development of accelerators (increased energy and intensity of the stable primary beams) and magnetic techniques (superferric quadrupole and superconducting quadrupole) have greatly improved the intensity of the radioactive fragments [GEI87, KUB03]. In 2015, more than 10 fragment separators are in operation in the world in different laboratories (FLNR, GANIL, GSI, Lanzhou, NSCL, RIKEN, ...)

4.2.1 First section: $B\rho$ dispersion ($R_{16} \neq 0$) and selection

The first stage of a fragment separator is a magnetic spectrometer, which selects ions according to their $B\rho$.

- The primary beam is sharply focused on the production target (area $\sim 2\text{-}3\text{ mm}^2$), the fragments of interest emerge from this point source.

- The fragments are focused (by quadrupoles), guided and analyzed (with a magnetic dipole).

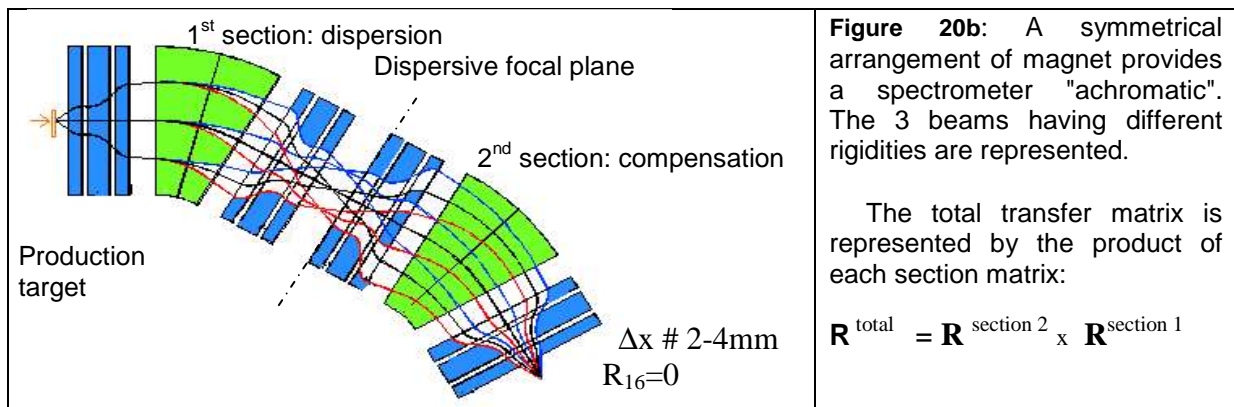


This section ensures the elimination of the primary beam particles. This allows to achieve a selectivity around 10^7 . This selection is in practice performed with slits located at the end of this section. The slit width is adjustable (with right and left movable plates). For some experiments, it is important to select a “Bp -window” to realize a compromise between purity and intensity.

It should be noted that the particles of interest are dispersed in an area related to their energy dispersion (in Bp) that can represent of up to $(100 * 50) \text{ mm}^2$. For nuclear physics studies of a single isotope, it is mandatory to refocus the beam (narrower spot) and to eliminate the unwanted ions.

4.2.2 2nd Section: dispersion compensating section ($R_{16}=0$)

The second stage is generally a symmetric copy of the first section, and it cancels the dispersion ($R_{16} = 0$). This has the advantage to refocus the particles of interest irrespective to their magnetic rigidity.



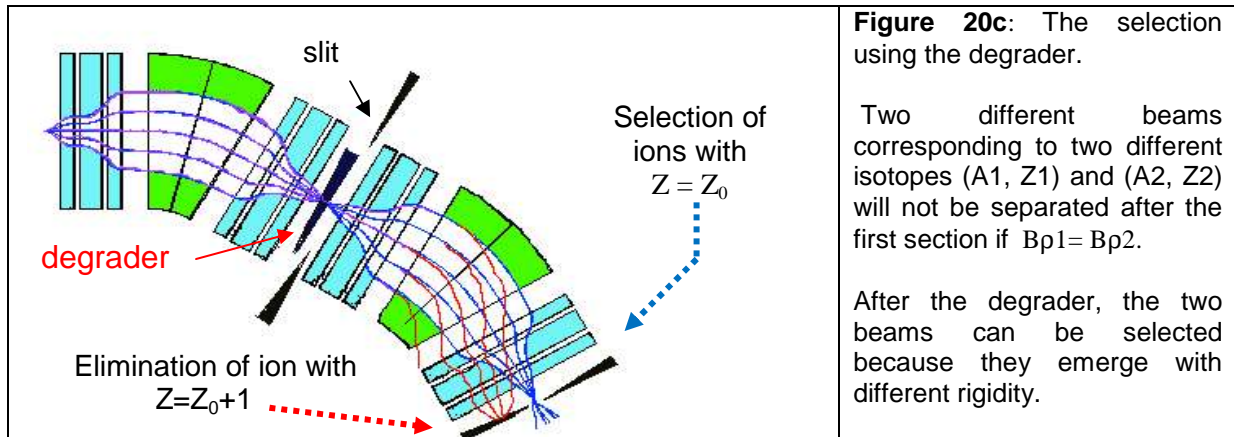
The matrix product of each section allows the computation of the total dispersion, which is zero in fragment separators: $R_{16}(\text{total}) = R_{11}^{\text{section 2}} R_{16}^{\text{section 1}} + R_{16}^{\text{section 2}} = 0$

Such an arrangement is however not satisfactory: a lot of reaction products are created in the fragmentation process, from $Z=1$ (proton) to $Z=Z_{\text{projectile}}$, so that the beam of interest is polluted by many other species (**Figure 21a**). An additional selection, which permits to select ions with a given atomic number (Z), has been optimized in the 1980s....

4.2.3 The second section and the selection with a degrader

The insertion of a thin foil in the intermediate focal plane (at the end of the 1st section) allows a selection that depends on the Z of the incident ions. Indeed, the ion energy loss in the degrader is dependent on the incident energy E, Z and A. More precisely, the Bethe-Bloch formula gives the ion energy loss in a given material:

$$\Delta E = k \Delta x (Z^2/A) (1/E)$$



Two different nuclei (A1, Z1) and (A2, Z2) having the same $B\rho$ arrive at the same position after the 1st stage. When crossing the degrader, their energy loss will depend on their atomic number Z, and one of the two nuclei can be selected. The 2nd section ensures with the an additional selection.

If the shape is not properly adjusted, it degrades the optical quality of the beam: two identical particles (A, Z and Q given), but with different $B\rho$, can be focused at the end of second section only if their relative difference in $B\rho$ at the entrance and exit of the is kept constant. So generally the thickness is not uniform in X: it must be thicker for larger $B\rho$. (see APPENDIX)

4.2.4 The identification in a fragment separator

The identification of the nuclei at the exit of the separator is made in two steps (ΔE , ToF).

- ΔE measurement (in a thin silicon detector)

This measurement identifies the Z of the fragments for a given A, because the energy loss ΔE is $\Delta E \sim k Z^2/A$

- Time of flight measurement (ToF)

The ToF is a measurement of the velocity, which is equivalent to a measurement of A / Q:

$$B\rho = \gamma v (A / Q)$$

The reference rigidity $B\rho_{ref}$ is fixed by the separator, so $B\rho = B\rho_{ref} (1 \pm \Delta)$ where Δ is in the acceptance in $B\rho$.

Assuming that the flight length L is constant whatever the $B\rho$ of the particles:

$$\Rightarrow A/Q = B\rho_{ref} (1 \pm \Delta) \cdot L / \text{ToF}, \text{ so } A/Q \sim k \text{ ToF} (1 \pm \Delta)$$

The uncertainty Δ prevents to identify isotopes with heavy masses, since the resolution is not always good enough: $R = \Delta > 1/A$

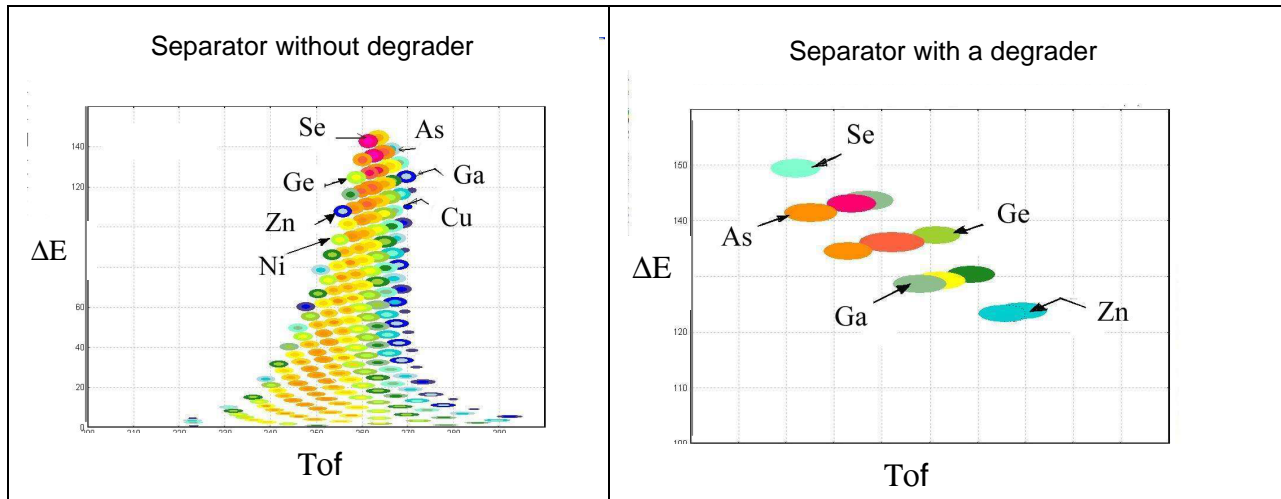


Figure 21a and 21b: Z identification with the Lise++ code [21] , corresponding to the fragmentation of ^{86}Kr @140 MeV/A to get ^{80}Ge .

- a) Without degrader, the fragment separator provides ions from selenium isotopes to protons.
 b) With a degrader the purity is improved. With the Identification in ΔE ($\sim Z$) and the time of flight (ToF $\sim A/Q$), each isotope appears a spot in the (ΔE , ToF) spectrum.

4.2.6 B_p tagging in modern fragment separators

The precision of the “A/Q” determination is connected to the acceptance in B_p of the separator. For better identification, it is sometimes necessary to close mobile slits to reduce the acceptance and to identify clearly the different ions $A-1$, A , $A+1$.

$$B_p = v (A/Q) \Rightarrow A/Q = B_p (1 \pm \Delta) / v$$

Unfortunately the reduction of the B_p acceptance to achieve a better identification, also reduces the available intensity for a given nucleus...A better idea, in modern fragment separators is to measure the A/Q ratio: it is derived from the B_p measurement performed in the dispersive focal plane using a position sensitive detector and from the time of flight.

B_p tagging with position measurement:

$$B_p = B_{p_{ref}} (1 + X / R_{16})$$

Velocity reconstruction with ToF measurement:

$$v = L / \text{ToF}$$

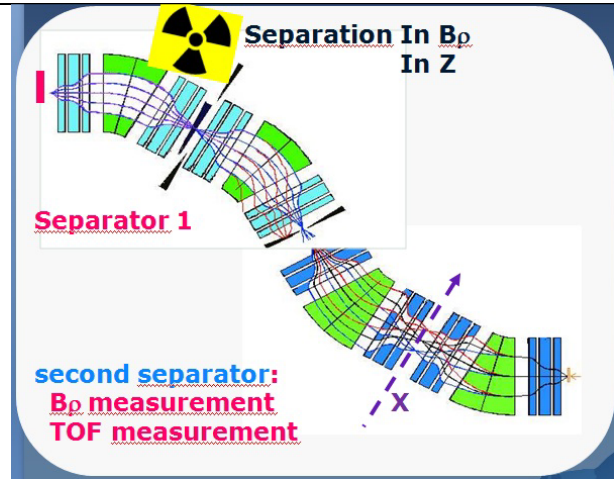
$$\Rightarrow A/Q = B_p / (\gamma V)$$

However the insertion of a position sensitive detector at the first intermediate focal plane is not always possible since the beam intensity is generally too high at this location...The construction of an additional achromatic separator can permit to install a q detector to perform the required B_p measurement. Besides, the second separator can improve the selection since a second degrader could be used in the dispersive focal plane (fig 22).

Figure 22: The first dispersive focal plane is not adapted for a particle detector because of the high beam intensity:

So a **second fragment separator** is needed to permit the B_p tagging. The position detector is installed in the second dispersive focal plane (where the dispersion is large $R_{16} \neq 0$) so

$$B_p = B_{p_{ref}} (1 + X / R_{16})$$



The superconducting separator BigRIPS [KUB03] has been designed for the RI-beam factory project at RIKEN. The BigRIPS separator is characterized by a large acceptance (large aperture quad) and a two-stage separator (A+B) scheme. It delivers purified and tagged RI beams.

Figure 23: B_p tagging at BIGRIPS

Achromatic separator A (F0-F2): (called the pre-separator)

- F0-F1: B_p selection ($R_{16} \neq 0$ in F1)
-
- F1-F2: R_{16} compensation ($R_{16} = 0$ in F2)

Achromatic separator B (F3-F7)

- section F3-F5: B_p dispersion
- 2nd degrader possible
- B_p measurement with a position sensitive detector in F5 ($R_{16} \neq 0$ in F5)
- section F5-F7: compensation ($R_{16} = 0$ in F7)

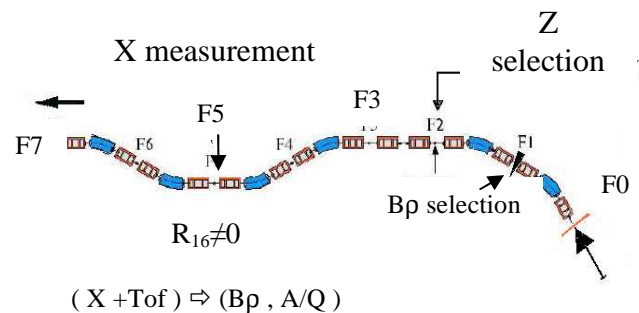
The identification relies on 3 measurements (ToF, ΔE , x)

A/Q is given by

$$A/Q \sim B_{pref} \cdot ToF$$

The Z identification is given by the energy loss ΔE in a silicon detector:

$$\text{since } \Delta E \sim K Z^2 / A$$



BigRips geometry at Riken (Tokyo), in operation since 2007.

- Pre-separator from F0, the target location, to F2:
(qqq B qqq). (qqq B qqq)
is in F1, but the Z selection is done with slits at F2
- Transition F2-F3: (qqq qqq)
- Separator From F3 to F7 (tagging)
(qqq B qqq qqq B qqq) . (qqq B qqq qqq B qqq)

Globally: 6 dipoles (30° and R=6m)
52 superferric quadrupoles

4.2.7 Fragment separators in the world

Separators	Lise3@Ganil	FRS GSI Optical mode N°1	A1900 MSU //NSCL	BIGRIPS @Riken
Geometry	(qqBqq)×2 + transfer line + (2 Wien filters)	(qqqBqqq+ qqqBqqq) ×2	(qqqBqqq+ qqqBqqq) ×2	(qqqBqqq qqqBqqq) ×3
Angular Acceptance	1.6 mstrd	3.4 mstrd	8 mstrd	10 mstrd
B _p Acceptance	± 2.5%	± 2.0%	± 3.0%	± 3.0%
Dispersion (R ₁₆)	1.7 m=1.7 cm/%	6.8 m=6.8 cm/%	5.95 cm/%	3.3 cm/%
B _p resolution	1/600	1/160	1/2900	1/3300
total length	42 m	69 m	35 m	77 m
B _p max	3.2 T.m	8.6 T.m	6.3 T.m	7.0 T.m
Comments	B=45° R=2m Conventional quadrupoles	B=30° Conventional quadrupoles	B=45° Superferric quadrupoles	B=30° R=6m Superferric quadrupoles

4.3 High-energy spectrometers

The availability of relatively intense and pure Radioactive Ion Beams (RIB), produced by projectile fragmentation, opens up the possibility to realize nuclear reactions study with these ions (knockout, coulomb excitation, inelastic scattering, transfer reaction).

The principle thus requires several steps:

- Fragmentation in a production target
- Achromatic fragment separator for purification
- Identification in A/Q (by B_p tagging, and ToF measurement)
- Secondary reaction target
- High energy spectrometer.

The coupling of the high energy spectrometer with a fragment separator permits to perform many reaction studies with identified radioactive ions. Let us mention several powerful “separator + spectrometer” couplings:

Facility	Fragment separator	Spectrometer
NSCL	A1900	S800
Riken	Big Rips	SHARQA
Riken	Big Rips	Zero degree
Riken	Big Rips	SAMURAI

4.3.1 The “dispersion matching” optical mode in S800 or in SHARQA

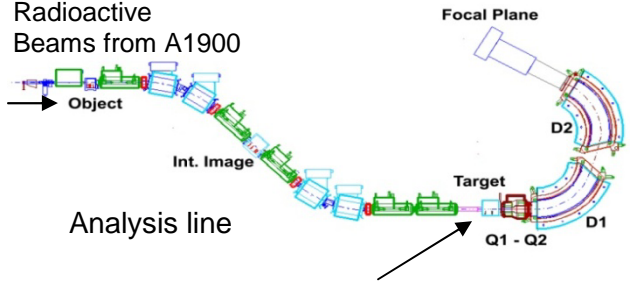
The dispersion matching mode is a technique used in several spectrometers, but it requires a long beam line with dipole magnets before the spectrometer itself. The radioactive beams produced by fragmentation have an important velocity dispersion ($\Delta v/v_0 > 3\%$). Using such beams for a secondary reaction leads to an important problem: since the momentum of the particle before the reaction is not known; it is not possible to determine the momentum transferred with a resolution better than $\Delta v/v_0$!

The solution is to adjust the dispersion with a beam line in such way that $R_{16} \neq 0$ on the target and $R_{16}=0$ in the focal plane of the spectrometer.

Such a dispersion matching mode is obtained with a specific tuning of the quadrupoles of the analysis line (fig. 24):

Analysis line + spectrometer: $R_{16}(\text{global})=0$
 Section 1: analysis line up to target, $R_{16}^{\text{analysis line}} \neq 0$
 Section 2: spectrometer, $R_{16}^{\text{spectrometer}} \neq 0$, but it compensates the analysis line
 $R^{\text{global}} = R^{\text{spectrometer}} \times R^{\text{analysis line}} \Rightarrow (R_{16}^{\text{final}} = R_{11}^{\text{spectrometer}} R_{16}^{\text{analysis line}} + R_{16}^{\text{spectrometer}} = 0)$

If there is no energy loss in the target, the particle is found at the exit of the spectrometer (the focal plane) at the central position $x_{\text{focal}} = 0$, whatever its initial momentum. If the particle has lost energy due to a nuclear reaction, the position is shifted $x_{\text{focal}} \neq 0$. The reconstruction of the momentum transferred is given by: $(P_f - P_i) / q = x_{\text{focal}} / R_{16}^{\text{spectrometer}}$



In the standard optical mode the dispersion is cancelled at the target position ($R_{16}^{\text{target}}=0$), but the dispersion matching mode is possible ($R_{16}^{\text{target}} \neq 0$ and $R_{16}^{\text{final}}=0$).

S800 :
 $R_{16}^{\text{spectro}} = 5 \text{ cm}/\%$

Fig 24: The S800 [BAZ03] at NSCL

The analysis line: This section of the S800 is used for different purposes, tuning the beam onto the reaction target, implementing various optical modes ($R_{16}^{\text{final}}=0$ or $R_{16}^{\text{final}} \neq 0$), as well as measuring the characteristics of the incoming particles.

S800 spectrometer: after the secondary target, the reaction products are measured and identified, the relatively large acceptance requires to take account optical aberrations:
 $B\rho = B\rho_0 (1 + x_f/R_{16} + a x_f^2 + b x_f'^2 + \dots)$

4.3.2 Several “high energy” spectrometers in the world

High energy Spectrometer	SHARQA @RIKEN [UES08] High Bp resolution	S800@ NSCL Good Bp resolution & large acceptance	Zero degree spectrometer @RIKEN
Geometry	Transfer line + target + qq B q B	Transfer line + target + qq B B	Target qqq B qqq
Rotation	-2° to +15°	0°-60°	0°
Optical modes	- dispersion matching (energy loss spectro.)	- standard - dispersion matching (energy loss spectro.)	- standard
Bpmax	6.8 T.m	4.0 T.m	6.8 T.m
Quadrupoles	Superferric quadrupoles		
Acceptance	2.7 mstrd	20 mstrd	~10 mstrd
Longueur	19.3m		
Magnetic dipole properties	B1 = 60° R = 4.4 m g = 200 mm B2 = 32.7° R = 4.4 m	B1 = B2 = 60°	B=30° R = 6 m = (6 cm/%)
Dispersion R_{16}	5.8 cm/% at target 0 cm/% at focal plane	5 cm/%	~2cm/%
Resolution in Bp	1/15000 (FWHM)	1/5000	1/2000

Other high energy spectrometers have been omitted, for instance a storage ring can be considered as Time-of-Flight spectrometer [KLU04]....

5. SPECTROMETER TUNING AND DIAGNOSTICS

We will see in this section some practical aspects of the tuning of a spectrometer. The spectrometer setting consists in several phases we will discuss in this section. An overview of the different steps is given in the following table:

A. Preparatory phase (theory and simulation, before the experiment)

- Evaluation of the experiment feasibility (beam intensity evaluation, detector R&D....)
- Choice of the beam optics (setting of the quadrupoles) to get the focus at a specific point...
- Evaluation of the B_p of the ions of interest (several settings are often needed: B_p of primary beam, B_p of the products $n^{\circ}1$, $n^{\circ}2$ )

B. Magnetic dipole's field setting and quadrupole setting (during the experiment)

- set the dipole magnets (B measurement with NMR probes or hall probe to adjust the B_p)
- set the quadrupoles (theoretical values $G(i)$ are used, and scaling to get the right B_p)

C. Beam tuning using diagnostics (during the experiment)

- Check the primary beam on target using a faraday cup or beam current transformers
Beam Alignment, using profil monitors
- Correct the beam alignment using steerer magnets, to ensure that the beam center is in the middle of the line before the target

- Transport the primary beam up to the spectrometer's end, if possible
Check the alignment (with profil monitors) and adjust the steerer magnets
Check the position foci (with profil monitor) (expertise is required)

5.1 Preparatory phase (reaction model and optical simulation)

The evaluation of the experiment feasibility (beam intensity evaluation, detector R&D,...) is realized a long time before the experiment. The spectrometer simulation is important mainly to quantify the intensity of the reaction products since the spectrometer transmission can be very low. The "Lise++" code can be used in numerous cases for a quick & reliable estimation.

The evaluation of the B_p of the ions of interest have to be done using the reaction model which gives the proper ion velocity. For the most probable charge state $\langle q \rangle$ at the exit of reaction target, several "stripping models" can be used (as available for instance in the Lise++ simulation code)

The choice of the "beam optics" (optical mode):

The setting of the quadrupoles will define the optical mode of the spectrometer.

The beam optics simulation has been done by the spectrometer designers (beam physicists). The goal of setting is generally to adjust the foci in horizontal and vertical planes and the dispersion coefficient to the required value: Indeed, the dispersion coefficient can be adjusted with the quadrupoles located directly after a dipole magnet.

Generally the conditions $R_{12}=R_{34}=0$ are required to get a small beam spot, but with a beam having a large energy dispersion $R_{16}=0$ is as well needed. On the opposite, a large R_{16} is

required for precise $B\rho$ measurements (since the resolution is better with large dispersion R_{16}) or for $B\rho$ selection.

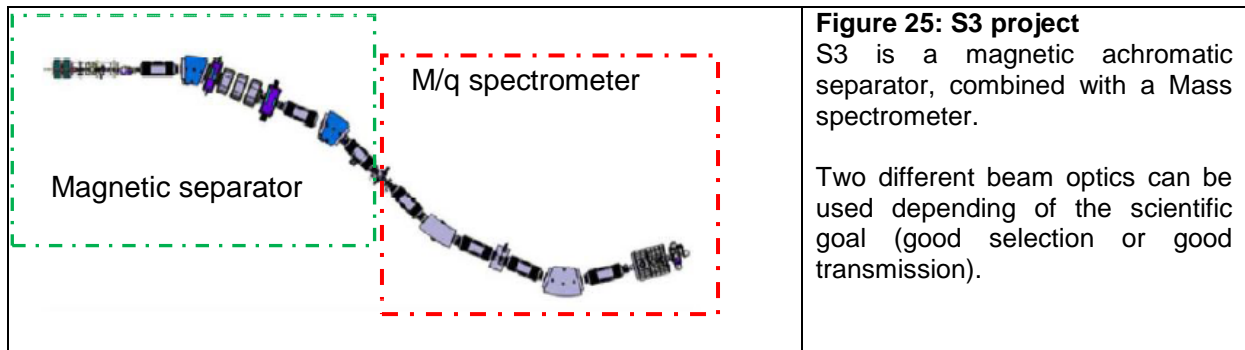


Figure 25: S3 project
 S3 is a magnetic achromatic separator, combined with a Mass spectrometer.
 Two different beam optics can be used depending of the scientific goal (good selection or good transmission).

In figure 26, two “beam optics” for 4 charge states of ^{102}Sn are presented for the S3 spectrometer project: (Lise++ code). The quadrupoles settings have been computed at $B_{\text{pref}}=1 \text{ T.m}$. The settings will be scaled depending on Br of the ions of interest...

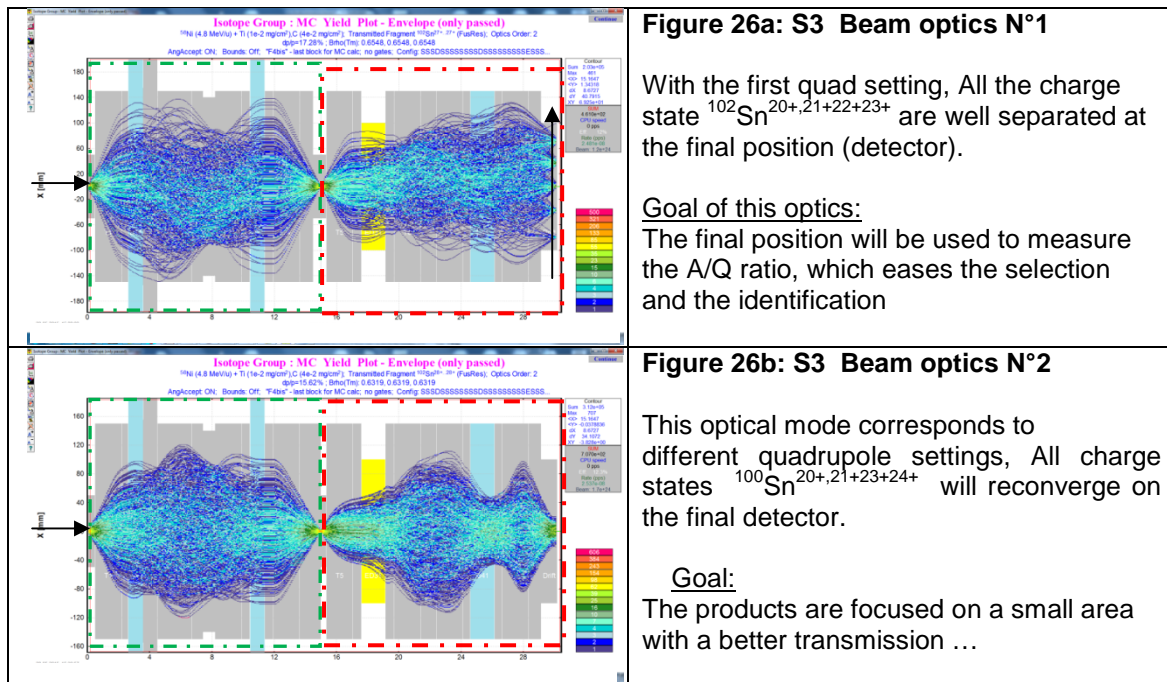


Figure 26a: S3 Beam optics N°1
 With the first quad setting, All the charge state $^{102}\text{Sn}^{20+,21+22+23+}$ are well separated at the final position (detector).
Goal of this optics:
 The final position will be used to measure the A/Q ratio, which eases the selection and the identification

Figure 26b: S3 Beam optics N°2
 This optical mode corresponds to different quadrupole settings, All charge states $^{100}\text{Sn}^{20+,21+23+24+}$ will reconverge on the final detector.
Goal:
 The products are focused on a small area with a better transmission ...

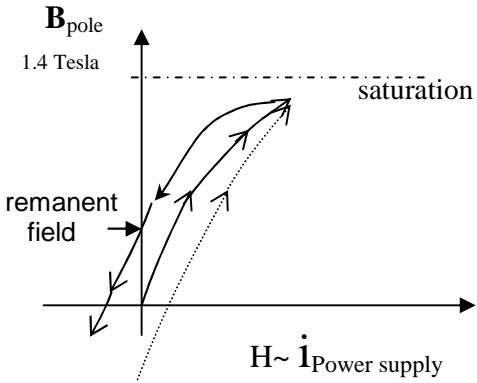
5.2 Magnetic dipole field setting and quadrupole setting

The setting of the power supply feeding the electromagnets (dipoles and quadrupoles) requires the knowledge of their magnetic properties:

For a dipole magnet, we compute the required field B_{dipole} for a given ion rigidity:

$$B_{\text{dipole}} = F(B\rho) = B\rho / R_{\text{dipole}}$$

Nota: The radius of curvature R_{dipole} of the reference trajectory is related to the deviation angle Φ , and the length of the magnet L_{eff} : $R_{\text{dipole}} = L_{\text{eff}} / \Phi$

<p>B(i) law in electromagnets:</p> <p>It gives the relationship between the magnetic field and the DC current of the power supply.</p>	<p>Setting the magnets:</p> <p>For dipole magnets: The field of the poles are related to the current of the associated power supply $B_{dipole} = f(i)$ ⇒ setting a magnet consists in adjusting “i” to get the required field: $i = i(B)$</p>
 <p>Hysteresis curve : starting from (i=0,B=0), then increase to $i = i_{max}$, then it is not possible to reach back the initial point (i=0,B=0) using the same current polarity.</p>	<p>Nota: Depending of the cycle of the magnet and on the temperature, a given current i can give different field values [hysteresis curve]. The dipole magnet setting with high precision requires to measure the field with NMR probes or Hall probes.</p> <p>For <u>quadrupole magnets</u>, the setting is done without field measurement. The curve Gradient = $f(i)$ should be known with good accuracy ($\sim 1\%$)</p> <p>Gradient = $2 \cdot B_{pole} / \text{Aperture} = f(i)$ Setting a quadrupole magnet to adjust “i” to get the required gradient: $i = i(\text{Gradient})$</p>

For a quadrupole, the gradient to be set for a given ion is related to the magnetic rigidity AND the desired beam optics (which defines the foci and dispersion): The “beam optics” in a spectrometer is generally computed for a given particle rigidity (the Reference magnetic rigidity $B_{p_{ref}}$).

So the beam optics is a list of the quadrupole gradients for ions having $B_p = B_{p_{ref}}$. In order to adjust the setting to the transport of a given ion, the gradients are scaled to the desired rigidities.

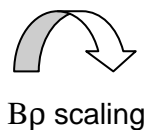
Example for the quadrupole setting of ions having $B_p = 1.5 \text{ T.m}$ with optical mode N°7xx:

Beam optics n°7xx :
Optics Name : focus at F_2

$B_{p_{ref}} = 1.00 \text{ T.m}$

Gq1 = 7.52 T/m
Gq2 = 12.15 T/m
Gq3 = 7.53 T/m
....

Beam optics simulation

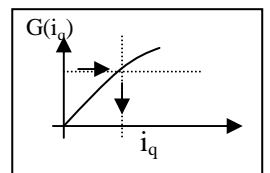


Quad settings for a beam with $B_p = 1.5 \text{ Tm}$
($B_p \neq B_{p_{ref}}$)

Beam optics n°7xx used

Quad GRADIENT	Power supply current
Gq1 = 7.52 T/m x ($B_p / B_{p_{ref}}$) = 11.28T/m	$i_{q1} = 55.2 \text{ A}$
Gq2 = 12.15 T/m x ($B_p / B_{p_{ref}}$) = 18.22 T/m	$i_{q2} = 77.1 \text{ A}$
Gq3 = 7.53 T/m x ($B_p / B_{p_{ref}}$) = 11.28T/m	$i_{q1} = 55.2 \text{ A}$
.....	

Quadrupole properties $G(i_q)$



5.3 Beam tuning using beam diagnostics

Beam diagnostics are essential tools of any accelerator and spectrometer. The beam diagnostics are dedicated robust detectors used for beam tuning purposes. The diagnostics give often access to statistical information about the beam (beam center $\langle x \rangle$ and $\langle y \rangle$, beam size σ_x, σ_y ; average intensity $\langle I \rangle$; bunch spread $\sigma_\tau \dots$)

Beam diagnostics is a rich field. A great variety of physical effects are made use of. We concentrate here on the most common devices used in the operation of a spectrometer [FOR06].

5.3.1 Current measurement with Faraday cups

The electrical current I_{beam} associated with the charged particle beam can be measured giving a measurement of the number of particle per second (if the charge of the particles is known).

The electrical current is

$$i_{\text{beam}} = dq/dt = Qe N / \Delta T$$

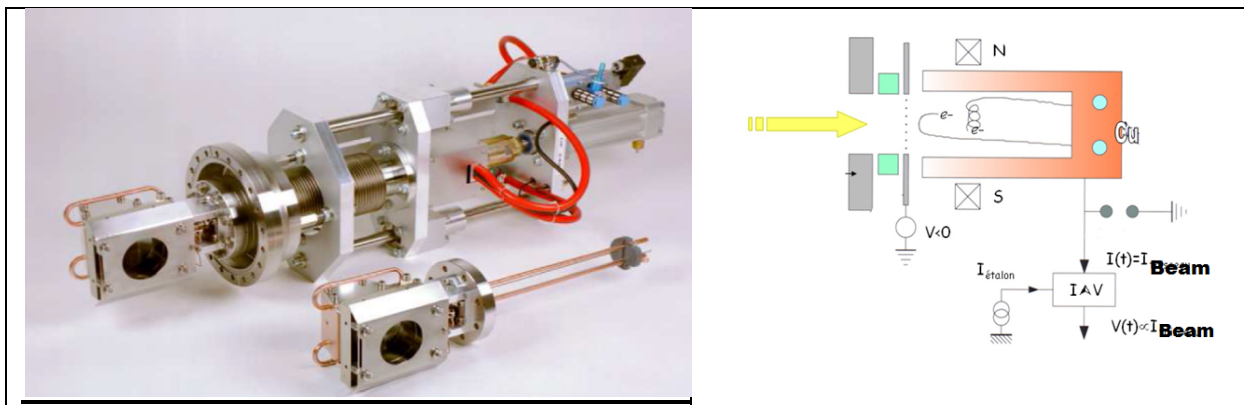
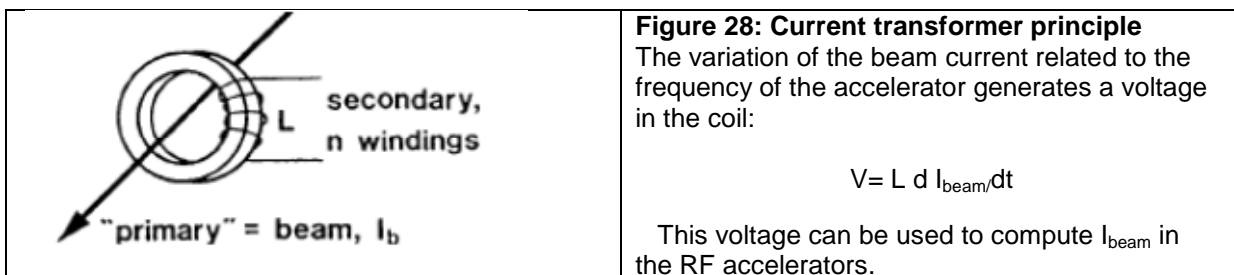


Figure 27: Faraday cup mounted on a feed-through (left). The technical scheme of a Faraday cup (right). The secondary emission can generate a lot of secondary electrons which can escape from the cup, changing the current measured. With magnets or high voltages, the charge can be confined in the copper cup.

5.3.2 Current measurement with current transformers

The beam current I_{beam} generates a magnetic field according to the Biot-Savart law. The effect of this very low magnetic field can be measured with bunched beams using current transformers.



The current transformers are well adapted to intense primary beams (beam current ranging from 0.1 μAe to 100 mAe) but not adapted for low intensity secondary ions.

5.3.3 Beam profil measurement

A large variety of devices can be used to evaluate the beam size in horizontal and vertical planes, the most used devices are:

- Secondary-Emission Monitors (wire monitors)
- Scintillator screens
- For low intensity beams ($I < 10^5 \text{pps}$) Micro Channel Plates can be as well used

Beam size measurement with a scintillator screen

The most direct way to observe a beam is the light emitted from a scintillation screen, monitored by a commercial video or CCD camera. These devices are installed in nearly all accelerators from the ion source up to the target. The scintillator screens are made often with a (Cr-doped) Al_2O_3 plate but many other materials can be used ($\text{Gd}_2\text{O}_2\text{S}$, CsI , SiO_2).

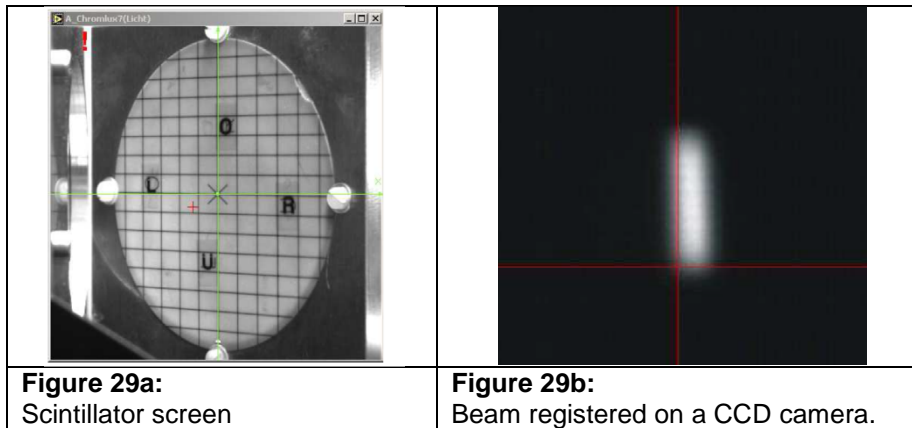


Figure 29a:
Scintillator screen

Figure 29b:
Beam registered on a CCD camera.

The wire profil monitor (Secondary-Emission Monitors)

An array of wires is inserted in the beam line. When the intercepting material (the wires) interacts with the beam, electrons are stripped from the surface of the wire. The more intense the beam intensity, the more intense the electron emission: The current emitted by each wire is registered and the **current measurements lead to the density profile of the beam.**

Reconstruct the beam intensity in X and Y

Profil monitor : HORIZ. and VERT. wire

Usefull for **beam alignment**
focusing check
R16 measurement

Figure 29: Multiwire profil monitors.

Transverse beam profiles obtained from the wires.

Top: 2 arrays of wires measure beam profiles in horizontal and vertical planes.

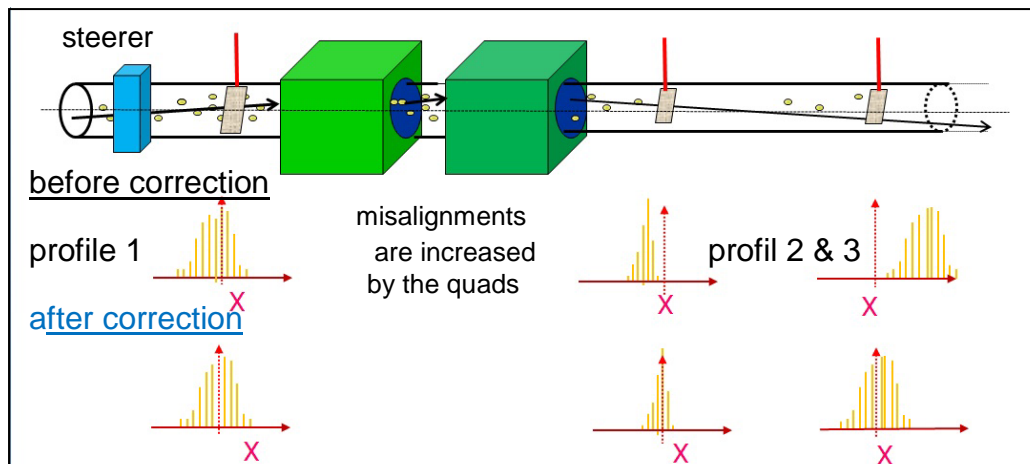
Bottom: The wire harps are mounted on a mobile device (*feed-through*) to be inserted in the beam line when it is needed.

A series of wire profile monitors help to check the beam alignment. These detectors are as well used for the commissioning of the different beam optics of a spectrometer: R₁₆ measurement, check of the foci in horizontal & vertical planes,...

The tuning of the beam in the spectrometer, will be done using the different diagnostics:

- Beam alignment, using profile monitors

There are several sections in the beam lines where the arrangement of several profile monitors and several steerer magnets can be used for the beam alignment. The beam centroid has to be set on the center of the beam line on each monitor using the correction magnets (steerers).



- Transport the primary beam up to the spectrometer's end

The tuning of the spectrometer with the primary beam allows checking the alignment and foci. Besides, it permits to check as well the identification detectors with a known beam (calibration purpose).

However the primary beam is too intense to be used directly on the particle detector. Therefore the beam intensity is reduced with a beam chopper or/and a pepper pot.

After checking the position of the foci (with profile monitors), one should report problems to the expert, if any: expertise is required for quadrupole's retuning and since the modification of the quad gradient change the dispersion and the focus at the same time, which is not desirable.

The magnetic field of the dipole and quadrupoles should then be rescaled for the desired fragment.

Check the primary beam on target:

The Day-to-day variations in transmission efficiency through an accelerator make the intensity unstable. As a consequence, the intensity's check is an important part of the beam tuning control. A Faraday cup or a beam transformer can be used to check the intensity on target during the experiment

6. CONCLUSION

We have seen in this lecture the elementary beam optical concepts needed to understand the use of spectrometers and separators in nuclear physics. We have discussed, the various separation techniques used in different ranges of ion energy (magnetic dipole, electrostatic deflector, gas filled separator).

The choice of a given technique for a specific experiment is the result of different compromises:

Selectivity versus Efficiency
Resolution versus Acceptance

The kinematics of the nuclear reactions of interest defines the main constraints for the design of a new spectrometer.

For the realization of a specific experiment, one must identify and answer the following questions:

- What quantities are needed for the experiment (angle, energy, velocity, mass)
- Is a spectrometer or separator really needed?
- What “accelerator+spectrometer” combination could be used in the world?
- What will be the spectrometer transmission for the product of interest?
- Which unwanted ions could reach the detector (pollution)?
- What is the maximum intensity of the primary and secondary beams? What are the induced problems: too high counting rates, thermal problem on target, radioactivity?

To go further in understanding spectrometers, I suggest the reading of the articles listed below

Bibliography:

Separation techniques for secondary ions

[MUN92] G. Münzenberg NIMB 70 (1992) 265-275

Large acceptance spectrometers

[SAV99] H Savajols et Al, Nucl Phys A 654 (1999)

[REJ08] M. Rejmund et A, NIMA 593 (2008) 343-352

Mass spectrometer RMS (Recoil Mass Spectrometer)

[COR83] T.M. Cormier et AL NIMB 212 (1983)

[IKE96] H. Ikezoe et Al, NIMA 376 (1996) 420-426

[JIN04] A. Jingan et Al , NIMA 526 (2004) 376-385

Gas-filled separators

[LEI99] Leino et Al, NIMB (1999), 653

[PAU89] M. Paul 1989 ,NIMA 277 , 418

[SAR11] J. Saren et Al. , NIMA 654 (2011) 508–521

High-energy spectrometer

[UE08] Sharaq ,T.Uesaka et Al Nim B 266 (2008) 4690-465

[BAZ03] S800, D.Bazin B 204 (2003) 629-633:

Fragment separators

[ANN87] R.Anne, D.Bazin, A.C.Mueller, J.C.Jacmart and M.Langevin, "The achromatic spectrometer LISE at GANIL", NIM A257 (1987) 215-232.

[GEI95] H.Geissel, G.Munzenberg, K.Riisager, "Secondary exotic nuclear beams", Annu. Rev. Nucl. Part. Sci. 45 (1995) 163-203.

[KUB03] BIG RIPS, Kubo et Al, NIMB 204 (2003) 97-113

Time-of-flight spectrometers

[KLU04] ESR Storage ring at GSI, H.J Kluge et Al., NIMA 532 (2004), 48-55

[WOO85] isochrone spectroTOFI, J.M. Wooter et Al. NIMA 240 (1985), 77-90

Lise++ Simulation

[TAR04] O. Tarasov, D. Bazin, Nucl Phys A 746 (2004) 411

Beam diagnostics

[FOR06] Peter Forck: Joint University Accelerator School 2006

Beam Stripping

[SCH01] Schiwietz-Grange, Nim B175, (2001) 125-131

I warmly thank all my colleagues from the different laboratories in the world for the documents they provided to me. I am most grateful to Jean-Charles Thomas for his time in reading and for his numerous suggestions about this lecture.

I also thank my colleagues at GANIL, who help me improving the presentation and the manuscript (Catherina Michelagnoli, Omar Kamalou, Yung hee Kim, Navin Alahari,...) .

APPENDIX

- APPENDIX 1: LISE++ simulation code**
- APPENDIX 2: Numerical integration of the equations of motion**
- APPENDIX 3: The quadrupole matrix**
- APPENDIX 4: Ion stripping in solid targets**
- APPENDIX 5: Wedge shape of the degrader**
- APPENDIX 6: Emittance evolution in a beam line**
- APPENDIX 7: Focusing in bending magnets**

APPENDIX 1: LISE++ simulation code

(O. Tarasov - D. Bazin [TAR03])

The Lise++ program is a key tool to study and simulate nuclear physics experiments with spectrometers; It includes dozens of tools and is downloadable for free.

- <http://www.ganil.fr/lise/proglise.html> (Web site lise GANIL)
- <ftp://ftp.nslc.msu.edu/lise> (Oleg Tarasov @MSU)

Lise++ includes in particular

- Calculation of ion charge state distributions
- Calculation of energy losses in materials (even a complex set of materials)
- Consideration of reaction kinematics
- Production of radioactive beams by in-light fragmentation, fusion-evaporation, fission
- Simulation of fragment separators (Bp, , ...)
- Pre-programmed configurations of existing separators Lise3, BigRips, A1900, FRS
- Simulation of new spectrometers

Exercise:

Simulate the fragmentation of a beam $^{78}\text{Kr}^{36+}$ at GANIL using the Lise spectrometer to produce ^{74}Kr :

0) Start Lise++

- 1) Load the configuration file of the separator: file/config/load/ganil/lise.lcn
- 2) Select the fragmentation reaction mechanism: Option/production mechanism/fragmentation
- 3) Define the projectile: [top, right click] and define $^{78}\text{Kr}^{36+}$ @ 75 MeV/A
Power=1.0 Kilowatt

4) Select the ion of interest: ^{74}Kr (Z=36)

5) Define the production target (carbon 100 microns): top right, click on target, then PT select carbon, then adjust the thickness in μm .

6) Compute the Bp of the desired ion and tune the spectrometer:

Experiment setting/optics/tune the spectrometer for the desired fragment

7) Compute the production of ^{74}Kr : Calculation/transmission&rate/one nucleus

Done !

Result: Intensity = $1.4 \cdot 10^5$ pps at the separator exit, but the beam is polluted. Add a degrader (wedge) in aluminium and restart the exercise.

Lise++ window

Projectile selection
Fragment selection
Target definition

« physical calculator »:
allows the calculation of Bp
, Ep, velocity, energy
loss.....

APPENDIX 2: Numerical integration of the equations of motion

The integration of particle's equation can be obtained with numerical methods. The equation to be solved is an "initial value problem" of Ordinary Differential Equations (ODE).

The « Newton-Lorentz » equation is our equation to be integrated: $\frac{d}{dt}[m\gamma \mathbf{v}] = q \cdot (\mathbf{v} \times \mathbf{B})$

We will use a Cartesian frame (x,y,z) for simplicity...

Expressing the vector product:

$$\mathbf{v} \times \mathbf{B} = \begin{vmatrix} \mathbf{e}_x & \mathbf{e}_y & \mathbf{e}_z \\ \dot{x} & \dot{y} & \dot{z} \\ B_x & B_y & B_z \end{vmatrix}$$

with the notation: $\frac{dx}{dt} = \dot{x}$

We obtain the 3 equations:

$$\frac{d}{dt}[m\gamma \dot{x}] = q(\dot{y} B_z - \dot{z} B_y)$$

$$\frac{d}{dt}[m\gamma \dot{y}] = q(\dot{z} B_x - \dot{x} B_z)$$

$$\frac{d}{dt}[m\gamma \dot{z}] = q(\dot{x} B_y - \dot{y} B_x)$$

This system of 3 second order differential equations (it contains second order derivative \ddot{x}). We want to re-formulate the 3 equations as a system of 6 first order ODE.

Besides, instead of the time evolution t , we will consider "z" as key parameter. ($\frac{d}{dz} x(z) = \dots$)

We remark that $\frac{d}{dt} = \frac{\dot{z}}{z} \frac{d}{dz}$ so, we have $\frac{d\mathbf{p}}{ds} = \frac{q}{\dot{z}} \cdot (\mathbf{E} + \mathbf{v} \times \mathbf{B})$

$$\frac{\dot{x}}{\dot{z}} = \frac{dx}{dz} = x' \quad \frac{\dot{y}}{\dot{z}} = \frac{dy}{dz} = y'$$

So we get the Momentum evolution

$$\frac{d}{dz}[m\gamma \dot{x}] = \frac{d}{dz} p_x = px' = q(y' B_z - \dot{z} B_y)$$

$$\frac{d}{dz}[m\gamma \dot{y}] = \frac{d}{dz} p_y = py' = q(\dot{z} B_x - x' B_z)$$

$$\frac{d}{dz}[m\gamma \dot{z}] = \frac{d}{dz} p_z = pz' = q(x' B_y - y' B_x)$$

And Position evolution

$$x' = \frac{dx}{dz} = \tan \theta = \frac{p_x}{p_z}$$

$$y' = \frac{dy}{dz} = \frac{p_y}{p_z}$$

$$z' = \frac{dz}{dz} = 1$$

Knowing the momentum $p_x(z)$ of a particle, let's express the momentum few mm's farther in the beam line. We express $p_x(z+dz)$ as a Taylor series:

$$p_x(z+dz) = p_x(z) + \frac{dp_x(z)}{dz} dz + \frac{dz^2}{2} \frac{d^2 p_x(z)}{dz^2} + \frac{dz^3}{3} \frac{d^3 p_x(z)}{dz^3} + \dots$$

The Euler's algorithm for this ODE system uses the first order approximation in the Taylor series:

The 6 equations are: $z(z = z_0 + dz) = z_0 + dz$

$$\begin{aligned}
 x(z = z_0 + dz) &= x_0 + \frac{dx}{dz} dz + 0(dz^2) & p_x(z) &= px_0 + \frac{dp_x}{dz} dz + 0(dz^2) \\
 -y(s = z_0 + dz) &= y_0 + \frac{dy}{dz} dz + 0(dz^2) & p_y(z) &= py_0 + \frac{dp_y}{dz} dz + 0(dz^2) \\
 & & p_z(z) &= pz_0 + \frac{dp_z}{dz} dz + 0(dz^2)
 \end{aligned}$$

The accuracy of such an approximation depends of the size on the small step dz , and the local error ε is proportional to $\varepsilon \sim dz^2$. Some more clever schemes reduce the errors, for instance the 4th order Runge Kutta method to has an error $\varepsilon \sim dz^4$.

Here, we present a tracking program for charged particles in a magnetic field:

```

Tracking program in a magnetic field: Euler algorithm (second order in Δz )
Initial coordinates and momentum for each particle at z=0 to be provided

X(Nparticle)= , Y(Nparticle)= , PX(Nparticle)= , PY(Nparticle)= , PZ(Nparticle)=

Magnetic field in 3D to be provided :

BX(x,y,z)= , BY(x,y,z)= , BZ(x,y,z)=

Loop j=1,Nparticle

z = 0      x = X(j), y = Y(j), p_x = PX(j), p_y = PY(j), p_z = PZ(j)

dz= 1 // (integration step 1mm)

Loop i=1,Nstep // step in dz

    B_x = BX(x, y, z)    B_y = BY(x, y, z)    B_z = BZ(x, y, z)

    x' = py / pz      y' = px / pz      z' = 1

    x = x + x' dz      y = y + y' dz

    p_x' = q (·B_x - x'·B_y)    p_y' = q (·B_x - x'·B_y)    p_z' = q (x'·B_y - y'·B_x)

    p_x = p_x + p_x' dz      p_y = p_y + p_y' dz      p_z = p_z + p_z' dz

Endloop i // end z-steps loop

Z(j) = i * Nstep      X(j) = x, Y(j) = y, PX(j) = p_x, PY(j) = p_y, PZ(j) = p_z

Endloop j // end particle loop

```

APPENDIX 3: The quadrupole matrix

Let's write the equation of motion in a magnetic quadrupole to get its optical matrix.

We could use a program to compute the trajectory of a specific ion (see APPENDIX 2), but we will see here that using few approximations the trajectory can be analytically derived.

We will describe the equation of the particle having the velocity $|\mathbf{v}|=v$, using a Cartesian coordinate system (x,y,z) , since the reference trajectory is a straight line.

We seek to compute the trajectory along the longitudinal axis z . For that purpose, we need to describe the transverse coordinates (x,y) as a function of z :

$$x = x(z)$$

$$y = y(z)$$

The Newton-Lorentz equation is:

$$\frac{d}{dt}[m\gamma \mathbf{v}] = q \cdot (\mathbf{v} \times \mathbf{B})$$

$$\frac{d}{dt}[m\gamma \dot{x}] = q(\dot{y} \cdot B_z - \dot{z} \cdot B_y)$$

$$\text{so } \frac{d}{dt}[m\gamma \dot{y}] = q(\dot{z} \cdot B_x - \dot{x} \cdot B_z)$$

$$\frac{d}{dt}[m\gamma \dot{z}] = q(\dot{x} \cdot B_y - \dot{y} \cdot B_x)$$

let's use the notation: $\frac{dx}{dt} = \dot{x}$

We want to transform the "t" parameter $x(t)$ as $x(z)$

$$\frac{d}{dt} = \frac{dz}{dt} \frac{d}{dz} = \dot{z} \frac{d}{dz} \quad \text{and the second derivative} \quad \frac{d^2 x}{dt^2} = \dot{z}^2 \frac{d^2 x}{dz^2} + \frac{d^2 z}{dt^2} \frac{dx}{dt}$$

- If the angles ($dx/dz = x'$ and $dy/dz = y'$) are small, $\frac{dz}{dt} = \dot{z} \approx v$

- If we consider the absence of electric field ($\mathbf{E}=0$, $|\mathbf{v}|=Cte$ and $\gamma=Cte$), we get $\frac{d^2 z}{dt^2} = 0$

How to Prove that: $\frac{dz}{dt} = \dot{z} \approx v$ and $\frac{d^2 z}{dt^2} = 0$?

Let's express dz/dt first:

When a particle travels a distance dz in the longitudinal axis, the flight length dL is:

$$dL_{\text{Flight}} = \sqrt{dz^2 + dx^2 + dy^2} = dz \cdot \sqrt{1 + (dx/dz)^2 + (dy/dz)^2}$$

$dx/dz = x'$ is related to the angle θ in the horizontal plan:

$$dx/dz = x' = \tan \theta$$

x' and y' are generally small (typically $x', y' < 0.01$ rad) and $dL_{\text{Flight}} \approx dz$.

So $\dot{z} = \frac{dz}{dt} \frac{dL}{dt} = \frac{dz}{dL} v \approx v + 0[(dx/dz)^2 + (dy/dz)^2]$

$$\text{and } \frac{d^2 z}{dt^2} = \frac{d \dot{z}}{dt} \approx \frac{dv}{dt} = 0 \quad (\text{since } \mathbf{E}=0 \Rightarrow |\mathbf{v}|=Cte)$$

The equations of motion are:

$$\frac{d}{dt} [m\gamma \dot{x}] = m\gamma \frac{d^2 x}{dt^2} = m\gamma \dot{z}^2 \frac{d^2 x}{dz^2} = -q \dot{z}^2 B_y + q \dot{y} B_z \quad \text{so} \quad m\gamma \dot{z}^2 \frac{d^2 x}{dz^2} = -q \dot{z} B_y + q \dot{y} B_z$$

$$\frac{d}{dt} [m\gamma \dot{y}] = m\gamma \frac{d^2 y}{dt^2} = m\gamma \dot{z}^2 \frac{d^2 y}{dz^2} = q(\dot{z} B_x - \dot{x} B_z) \quad m\gamma \dot{z}^2 \frac{d^2 y}{dz^2} = q(\dot{z} B_x - \dot{x} B_z)$$

Let's consider a quadrupolar field with a gradient G :
 $B_x = +Gy$
 $B_y = +Gx$
 $B_z = 0$

The equation appears after simplification ($\dot{z} \approx |\mathbf{v}|$) in a very simple form:

$$\frac{d^2 x}{dz^2} = -\frac{q}{m\gamma v} (B_y + \dot{y} B_z) \quad \frac{d^2 x}{dz^2} = -\frac{q}{m\gamma v} (B_y) = \left[-\frac{q}{m\gamma v} G x\right]$$

it leads to

$$\frac{d^2 y}{dz^2} = \frac{q}{m\gamma v} (\dot{B}_x - \dot{x} B_z) \quad \frac{d^2 y}{dz^2} = \frac{q}{m\gamma v} (B_x) = \frac{q}{m\gamma v} \cdot G y$$

With the approximation, the equations are the one of the harmonic oscillator:

$$\frac{d^2 x}{dz^2} + K_x x = 0 \quad \text{With} \quad K_x = k = \frac{q}{m\gamma v} G = -K_y$$

$$\frac{d^2 y}{dz^2} + K_y y = 0$$

$$m\gamma v/q = B\rho$$

If $K_x > 0 \Rightarrow K_y < 0$

We find that along x a particular solution is represented by a stable oscillation $x(z) \sim \exp(i\omega z)$ which corresponds to a focusing case. While along y, a solution is an exponential growth $y(z) \sim \exp(+\omega z)$: It corresponds to a diverging solution when $z \rightarrow \infty$ (defocusing case).

The general solution $x(z)$ can be expressed as a function of the initial coordinates (x_0, x_0') at the entrance of the quadrupole:

$$x(z) = x_0 \cos(\sqrt{k}z) + x_0' \frac{1}{\sqrt{k}} \sin(\sqrt{k}z)$$

$$x'(z) = \frac{dx}{dz} = -x_0 \sqrt{k} \sin(\sqrt{k}z) + x_0' \cos(\sqrt{k}z)$$

Using a (2x2) matrix notation, x and $x' = dx/dz$ can then be written as follows:

$$\begin{pmatrix} x(z) \\ x'(z) \end{pmatrix} = \begin{pmatrix} \cos(\sqrt{k}z) & \frac{1}{\sqrt{k}} \sin(\sqrt{k}z) \\ -\sqrt{k} \sin(\sqrt{k}z) & \cos(\sqrt{k}z) \end{pmatrix} \cdot \begin{pmatrix} x(z_0) \\ x'(z_0) \end{pmatrix} = \mathbf{M}_x \cdot \begin{pmatrix} x(z_0) \\ x'(z_0) \end{pmatrix}, \quad \text{this is the focusing part.}$$

Let us remark that we have $\det \mathbf{M}_x = 1$, which is related to the Liouville theorem...

For the vertical plane, the diverging solution for large z corresponds to a defocusing, as a general solution $y(z)$, we have:

$$\begin{pmatrix} y(z) \\ y'(z) \end{pmatrix} = \begin{pmatrix} \cosh(\sqrt{k}z) & \frac{1}{\sqrt{k}} \sinh(\sqrt{k}z) \\ \sqrt{k} \sinh(\sqrt{k}z) & \cosh(\sqrt{k}z) \end{pmatrix} \cdot \begin{pmatrix} y(z_0) \\ y'(z_0) \end{pmatrix} = \mathbf{M}_y \cdot \begin{pmatrix} y(z_0) \\ y'(z_0) \end{pmatrix}, \text{ this is the defocusing part.}$$

Using the six dimension matrix notation, the transfer matrix of a quadrupole (horizontal focusing) of length L is:

$$\begin{bmatrix} x \\ x' \\ y \\ y' \\ l \\ \delta \end{bmatrix}_{z=L} = \begin{bmatrix} \cos(\sqrt{k}L) & \frac{\sin(\sqrt{k}L)}{\sqrt{k}} & 0 & 0 & 0 & 0 \\ -\sqrt{k} \sin(\sqrt{k}L) & \cos(\sqrt{k}L) & 0 & 0 & 0 & 0 \\ 0 & 0 & \cosh(\sqrt{k}L) & \frac{\sinh(\sqrt{k}L)}{\sqrt{k}} & 0 & 0 \\ 0 & 0 & +\sqrt{k} \sinh(\sqrt{k}L) & \cosh(\sqrt{k}L) & 0 & 0 \\ 0 & 0 & 0 & 0 & 1 & L/\gamma^2 \\ 0 & 0 & 0 & 0 & 0 & 1 \end{bmatrix} \cdot \begin{bmatrix} x_0 \\ x'_0 \\ y_0 \\ y'_0 \\ l_0 \\ \delta_0 \end{bmatrix}_{z=0} \quad \text{With } k = \frac{G}{B\rho} G$$

This matrix model is used to describe the particle dynamics in any quadrupole with $k = \text{Gradient}/B\rho_{\text{ref}} > 0$ (horizontal focusing).

For a quadrupole of opposite polarity ($G < 0$), the vertical sub-matrix \mathbf{M}_y is exchanged with the horizontal sub-matrix \mathbf{M}_x .

Why does $R_{66} = 1$ in the quadrupole matrix?

A magnetic field does not change the momentum of an ion, so the magnetic rigidity remains constant in a magnetic quadrupole: $B\rho = B\rho_{\text{ref}} (1 + \delta_{\text{initial}}) = B\rho_{\text{ref}} (1 + \delta_{\text{final}})$ so $R_{66} = \frac{\partial \delta_{\text{final}}}{\partial \delta_{\text{initial}}} = 1$

Why does $R_{56} = (x|\delta) = L/\gamma^2$?

Let us note that in the for R_{56} coefficient, a relativistic factor γ^2 appears, like in a drift matrix. Actually after the quadrupole, the longitudinal difference l of two ions, with different $B\rho$ and travelling on the reference axis, is:

$l = v_0(t_1 - t_2)$ (t_1 and t_2 are the time of flight of the 2 ions, this is the definition of the l parameter)

Let's write the position difference of two ions (the reference one and a quicker ion, having respectively a velocity v_0 and v)

$$l = z_5 = -v_0(t - t_0) = -v_0 \left(\frac{L}{v} - \frac{L}{v_0} \right) = -v_0 L \left(\frac{v_0 - v}{vv_0} \right) = \frac{\Delta v}{v} L = \frac{\Delta \beta}{\beta} L = \frac{1}{\gamma^2} \frac{\Delta p}{p} L = \frac{L}{\gamma^2} \delta$$

$$\text{Since } \frac{dp}{d\beta} = \frac{d(m\gamma\beta c)}{d\beta} = \dots = \gamma^2 \frac{p}{\beta} \Rightarrow \frac{\Delta \beta}{\Delta p} = \frac{1}{\gamma^2} \frac{\beta}{p}$$

$$\text{so } R_{56} = (x|\delta) = \frac{\partial l}{\partial \delta} = L/\gamma^2$$

APPENDIX 4: Ion stripping in solid targets

Accurate predictions of the charge state distributions for heavy ions in solid material are particularly interesting for the design of new accelerators and for nuclear physics experiments (Bp estimate, primary beam charge state contaminations ...).

In a target, the atomic interaction results in electron exchanges between the projectile ion and the target atoms. The final charge state of the projectile follows a distribution probability $F(q)$ that looks like a Gaussian centered around a mean value $\langle q \rangle$ and with a width σ_q .

Physics of the stripping phenomena

The charge-state distribution of ions after passage in a solid target is a result of many atomic interactions resulting in:

- target electron capture by the projectile,
- Electron stripping.

The capture cross section dominates at low energy ($E < 0.5$ MeV/A) while the stripping becomes more and more important at higher energy.

<p style="text-align: center;">$\langle q \rangle = +27.2$</p>	<p>The charge distribution after target is characterized by the mean and width</p> $\langle q \rangle = \sum_{q=0}^{q=Z_{\text{projectile}}} q \cdot F(q)$ $\sigma_q^2 = \sum_{q=0}^{q=Z_{\text{projectile}}} (q - \langle q \rangle)^2 \cdot F(q)$ <p>The probability is normalized:</p> $1 = \sum_{q=0}^{q=Z_{\text{projectile}}} F(q)$
	<p>Processes involved in electron exchange reactions between the target atom and the projectile ion:</p> <p>The charge probability $F(q)$ obeys a master equation as a function of the target thickness T:</p> $\frac{dF(q)}{dT} = \sum_{q' \neq q} F(q') \sigma(q, q') - F(q) \sigma(q, q')$ <p>The charge exchange cross section $\sigma(q, q')$ exceeds typically 1 Mbarn.</p>

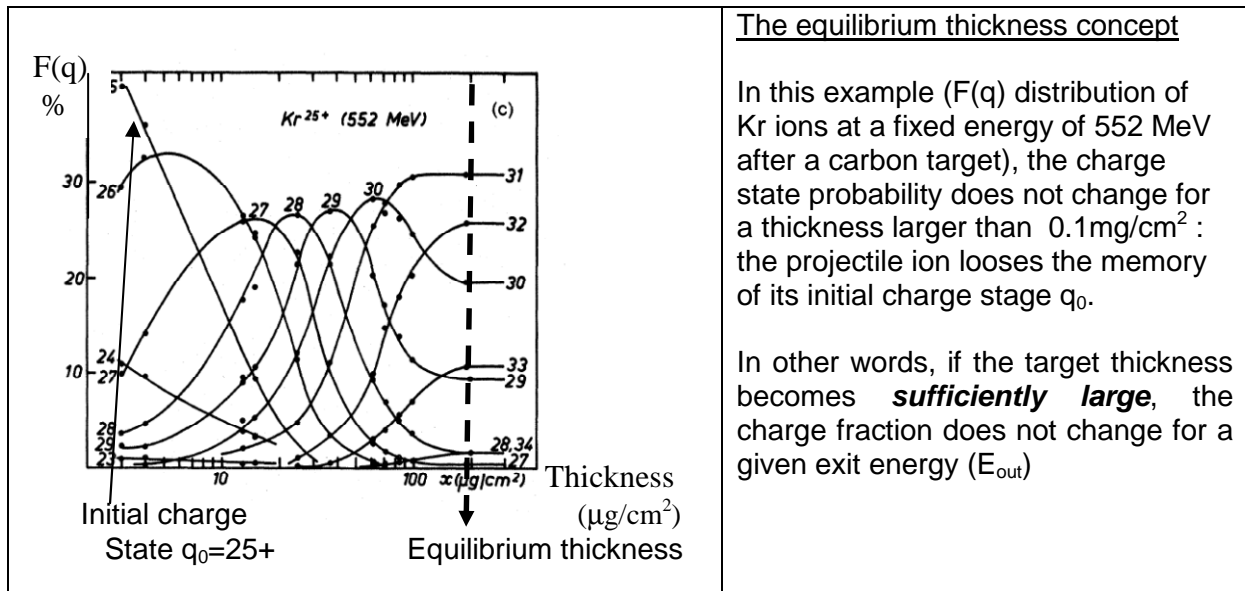
When heavy ions penetrate through matter, the atomic interaction between the projectile electrons and the target atoms results in considerable fluctuations of the ion charge state.

In general, the probability of finding an ion in a final charge state q' behind a target depends mainly on 3 parameters:

- the nuclear charge $Z_{\text{projectile}}$ of the projectile ions,
- the velocity v at the exit of the target,
- the nuclear charge Z_T of the target atoms.

If the target is thick enough (thicker than the equilibrium thickness):

- $F(q)$ does not depend on the initial charge state q_0 ,
- $F(q)$ depends weakly of target thickness T



Empirical models for $F(q)$

Charge-state distribution measurements have been reported for different ion energies and several authors have derived empirical formulae which are more or less modifications of the Betz formulae.

The simple "Betz formula"

Betz provided in 1983 one of the first simple and "rather accurate empirical model":

$$\langle q \rangle_{\text{Betz}} (Z, v_{\text{out}}, Z_{\text{Target}} = 6) = Z \cdot \left[1 - 1.041 \exp \left[-0.851 Z^{0.432} \cdot \left(\frac{v_{\text{out}}}{v_0} \right)^{0.847} \right] \right]$$

$$\sigma_{\text{Betz}} = 0.27 \cdot Z^{1/2}$$

where v_0 is the velocity of the electron in the orbital $\lambda=1$ ($v_0 = e^2/h = 2.188 \times 10^6 \text{ m/s}$).

Today it is recommended to use models based on the largest measurement databases:

- Schiwietz-Grange model for low energy ion ($E < 15 \text{ MeV/A}$) [**SCH04**]
- "Global" model for higher energy ion ($E > 30 \text{ MeV/A}$) [**NimB142,(1998)**]

The target dependency

Most of the models use carbon target measurements as a reference, but the use of target with higher atomic numbers ($Z_{\text{target}} > 6$), decreases the mean charge state $\langle q \rangle$ at low energy. Empirical models extrapolate in general the carbon foil stripper results:

$$\langle q \rangle (Z, v_{\text{out}}, Z_{\text{Target}} \neq 6) = \langle q \rangle (Z, v_{\text{out}}, Z_{\text{Target}} = 6) \cdot G(Z_{\text{target}})$$

Since it is better to have less charge states in the spectrometer, it is always desirable to try to have the highest charge state (i.e. $\langle q \rangle$ maximal).

The ideal case is fully stripped ions ($\langle q \rangle = q = Z$): in this case, the identification is simpler, and the possibility to get primary charge states at the Bp of interest is reduced.

The ideal target for stripping is a target with low Z, and low cost: the carbon foils are an excellent choice for nuclear physics experiment or accelerators. In physics experiments, carbon strippers are often used after the target to get the smallest charge state distribution with the highest mean charge state $\langle q \rangle$.

Equilibrium thickness with a carbon stripper for several beams:

Beam	Final energy MeV/A	equilibrium thickness in carbon Foil
^{12}C	4.3	0.050 mg/cm ²
^{12}C	10.0	0.110 mg/cm ²
^{40}Ar	4	0.150 mg/cm ²
^{40}Ar	10	0.400 mg/cm ²
^{238}U	3.8	0.250 mg/cm ²
^{238}U	11	1.00 mg/cm ²
^{238}U	15	1.4 mg/cm ²

Reliability of the empirical models

The mean charge state $\langle q \rangle$ predicted by the most recent models is rather accurate:

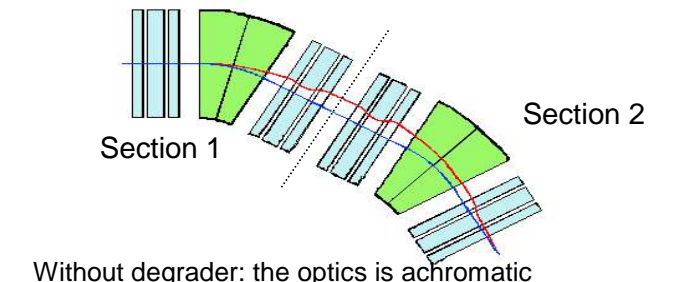
$$\langle q \rangle = \langle q \rangle_{\text{model}} \pm 1.$$

However, for very specific cases (very low energy or very specific target), in order to improve the prediction, it is always better to check the validity of a model in a case close to the experimental conditions (previous measurements or data available) and to compute the error of the model $\Delta q_{\text{correction}}$:

$$\langle q \rangle = \langle q_{\text{model}} \rangle + \Delta q_{\text{correction}}$$

APPENDIX 5: Wedge shape of the degrader

In the lecture, we learnt that a fragment separator is a 2 stage achromatic magnetic spectrometer ($(x|\delta)=R_{16}=0$). We demonstrate in this section that the degrader shape has to be optimized to preserve the achromaticity of the separator.

	<p>2-stage magnetic separator</p> <p>2 trajectories A and B , with 2 different $B\rho$ are represented: $Z_A(x_0=0, \theta_0=0, y_0=0, \phi_0=0, \delta=0)$ $Z_B(x_0=0, \theta_0=0, y_0=0, \phi_0=0, \delta=0.02)$</p> <p>The total transport matrix is achromatic $R_{16}(\text{total})=0$ since the two ions arrive at the same position in x plane.</p>
---	---

The total dispersion $R_{16}(\text{total})$ is cancelled by the compensation of the 2 sections. We can express this by the matrix product $\mathbf{R}(\text{total}) = \mathbf{R}^{\text{section 2}} \cdot \mathbf{R}^{\text{section 1}}$

So, as a result of the matrix product, we get:

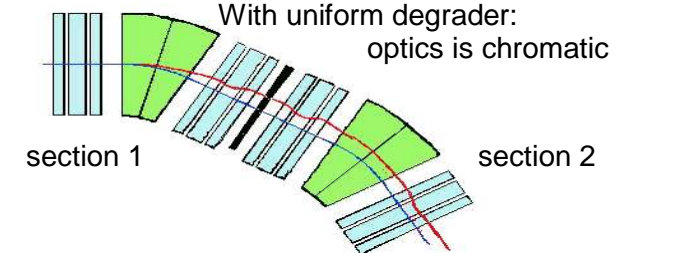
$$R_{16}(\text{total}) = R_{11}^{\text{section 2}} R_{16}^{\text{section 1}} + R_{16}^{\text{section 2}} = 0$$

Without degrader, the final position of the particle B (red) is $X_B=0$.

$$X_B = R_{16} \delta = 0 = R_{11}^{\text{section 2}} R_{16}^{\text{section 1}} \delta + R_{16}^{\text{section 2}} \delta$$

The goal of the degrader is to separate the different particles according to their Z (in order to separate the different isobars). If the shape of the degrader is not adjusted, it degrades the optical quality of the desired beam.

Two particles of the same type (A, Z and Q given), but with different $B\rho$, will re-converge towards the same point, if the relative difference in $B\rho$ at the entrance and exit of the degrader is the same.

	<p>A uniform degrader</p> <p>2 identical particles , with different $B\rho$ are represented: The red particle do not arrive at $x=0$: $X_B \neq 0$</p> <p>Why isn't the spectrometer any longer achromatic?</p>
---	---

The demonstration requires few lines, but the main reason is that the energy loss is energy dependent. For (A,Z) fixed, the Bethe Bloch formula for the energy loss in a degrader of thickness T reads:

$$\Delta E \sim K(A,Z) T / E, \quad \text{so } \Delta E/E \sim T / E^2$$

In a non relativistic approximation ($\Delta E/E=2\Delta v/v$ and $E^2 \sim v^4$), the velocity loss in the degrader is given by:

$$\Delta v/v = \Delta B\rho / B\rho = 0.5 \Delta E/E \sim T / B\rho^4 \quad (\text{Note the power 4 !!!})$$

Let's write the loss in magnetic rigidity with a uniform degrader of Thickness T:

$$\Delta B\rho = -\alpha \cdot T \cdot B\rho_{\text{ref}} \quad (\text{For the reference particle})$$

For the particle with $B\rho^B = B\rho_{ref} (1+\delta)$, $\Delta B\rho = -\alpha \cdot T \cdot B\rho_{ref} / (1+\delta)^4$

<p>Before the degrader (section 1):</p> $B\rho^A = B\rho_{ref}$ $B\rho^B = B\rho_{ref} (1+\delta)$ $[B\rho^B - B\rho^A] / B\rho^A = \delta$	<p>After the uniform degrader (section 2):</p> $B\rho^A = B\rho_{ref} (1 - \alpha T)$ $B\rho^B = B\rho_{ref} (1 + \delta - \alpha T / (1 + \delta)^4)$ $[B\rho^B - B\rho^A] / B\rho^A = \delta_2 \neq \delta$
---	---

We had $R_{11}^{section 2} R_{16}^{section 1} + R_{16}^{section 2} = 0$, so if the factor δ_2 is not equal to δ , the spectrometer is not any longer achromatic since:

$$X_B = R_{11}^{section 2} R_{16}^{section 1} \delta + R_{16}^{section 2} \delta_2 \neq 0$$

Therefore, the particle B does not re-converge toward the particle A.

We can use a non uniform degrader to obtain $X_B=0$.

The trick is to adjust the thickness in order to get relatively the same $B\rho$ difference before and after the degrader, so that $\delta_2 = \delta$
The 2 particles converge to the same point: $X_B = 0$ and $X_A=0$

Since

$$R_{11}^{section 2} R_{16}^{section 1} \delta + R_{16}^{section 2} \delta = 0$$

So by choosing a thickness like:

$$T = T_0 \cdot [1 + cx]$$

We can get:

$$X_B = R_{11}^{section 2} R_{16}^{section 1} \delta + R_{16}^{section 2} \delta = 0$$

PROOF:

After the degrader with the variable thickness, the two particles are slowed down:

$$B\rho^A = B\rho_{ref} (1 - \alpha T_0)$$

$$B\rho^B = B\rho_{ref} (1 + \delta - \alpha T_0 \cdot [1 + cx] / (1 + 4\delta)) + O(\delta^2)$$

at the degrader location we have $x = R_{16}^{section 1} \delta$

$$B\rho^B = B\rho_{ref} [1 + \delta - \alpha T_0 \cdot [1 + cx] / (1 + 4x / R_{16}^{section 1})]$$

A degrader, with a variable thickness conserves the achromaticity in the non relativistic approximation:

If $T(x) = T_0(1 + 4x / R_{16}^{section 1})$, we have

$$[B\rho^B - B\rho^A] / B\rho^A = \delta_2 = \delta \Rightarrow X_B = 0$$

This kind of degrader (not uniform in x) is called an **achromatic degrader**: it must be thicker for particles with larger $B\rho$.

	<p>A wedge shaped degrader</p> <p>2 identical particles with different $B\rho$ are represented</p> <p>The two particle arrive at the same horizontal position whatever their initial rigidities : $R_{16}=0$</p>
--	---

APPENDIX 6: emittance evolution in a beam line

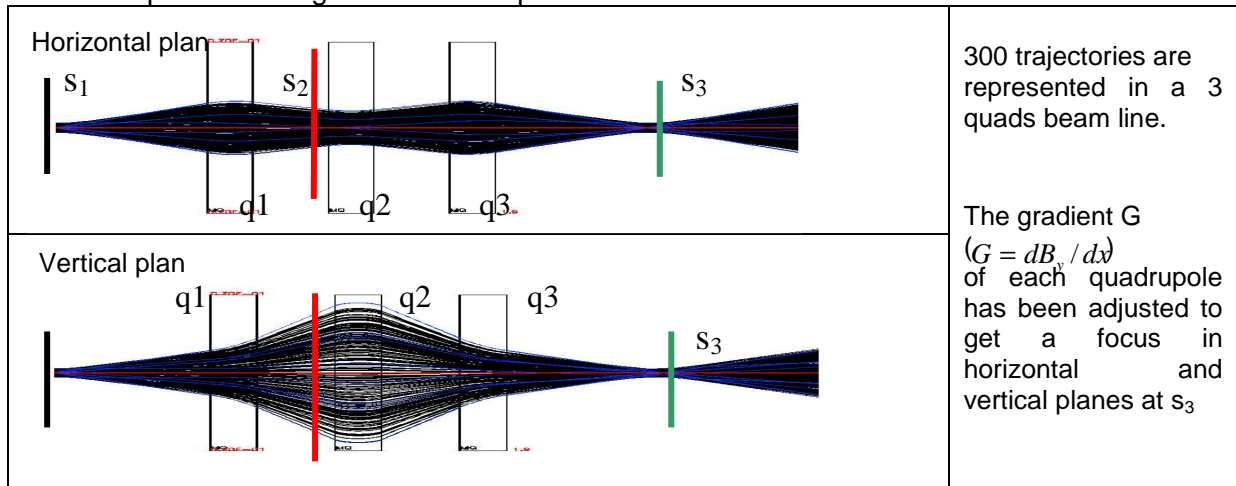
Let us study the effect of a quadrupole triplet in the transport of a charged particle beam in the context of a "point to point focusing".

Beam line: 3 magnetic quadrupoles, with a full aperture $\phi = 70$ mm and a length $L=300$ mm; beam line length = 3.9 m; space between quads=0.5m

The beam optics:

Point to point focusing in the horizontal plane (it starts with a focus and ends-up with a focus).

Point to point focusing in the vertical plane.



Remark: q1 and q3 focus in the horizontal dimension (while they defocus in vertical plane) q2 focus in the vertical plane

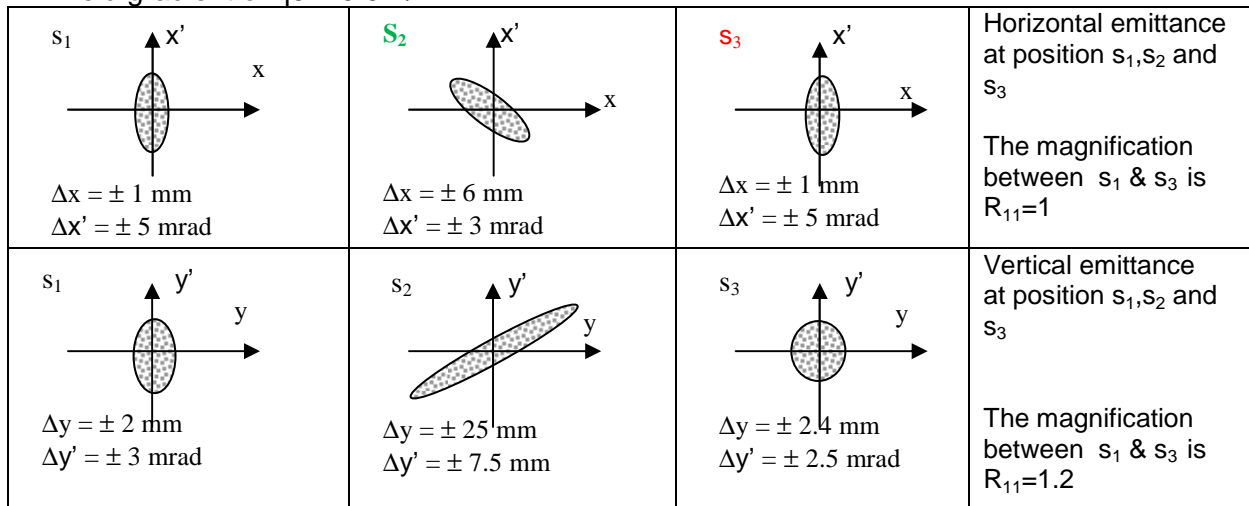
Simulation parameters: $B\rho(\text{beam}) = 1 \text{ T.m}$ ($^{12}\text{C}^{3+}$, $E=3.01 \text{ MeV/A}$), monochromatic:

$$\Delta v/v = \Delta B\rho/B\rho = 0$$

Field gradient of q1 = 4.725 T/m

Field gradient of q2 = - 6.117 T/m

Field gradient of q3 = 5.5 T/m



Emittance evolution: The ellipse area is kept constant in the horizontal & vertical planes, since the Liouville theorem holds in this context (the phase space volume is conserved with non dissipative forces). Remember that the horizontal angles correspond to $x'=dx/ds = \tan \theta \sim \theta$ and $y'=dy/ds = \tan \phi \sim \phi$.

APPENDIX 7: Focusing in bending magnets

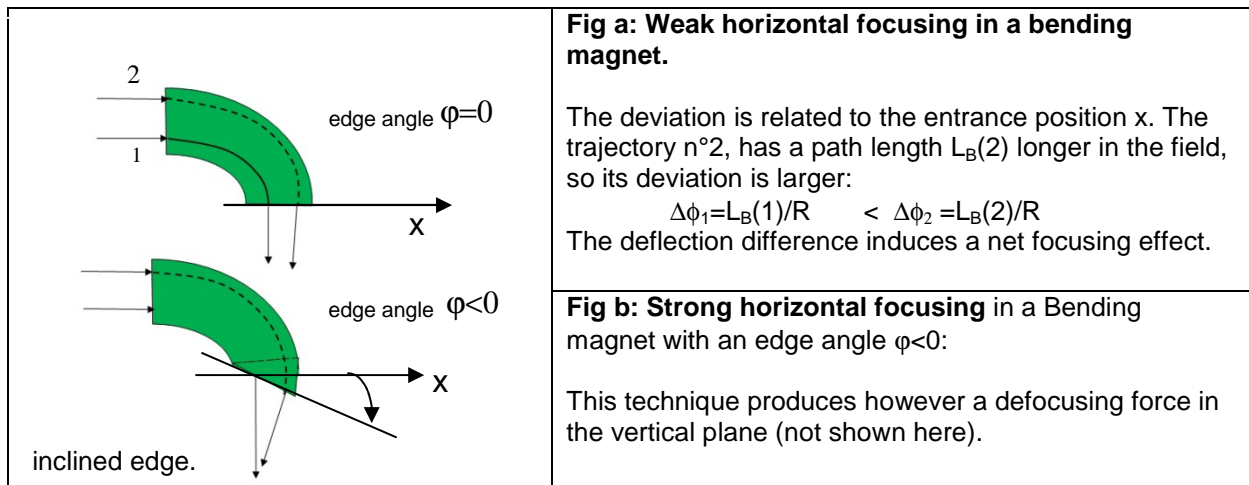
A dipole magnet bends the trajectories of charged particle, but it can focus as well the particles and complements the quadrupole magnets.

The focusing of a dipole magnet is related to shape of the poles: The dipole end's angles (the entrance and exit edges) produce an additive focusing effect. The focusing effect of bending magnets with inclined edges is useful in spectrometers and accelerators.

We shall see 3 cases:

- Weak horizontal focusing: Normal dipole magnet, with edges perpendicular to the trajectory,
- Strong horizontal focusing: A dipole magnet with a negative edge angle $\varphi < 0$,
- Horizontal defocusing: A dipole magnet with a positive edge angle $\varphi > 0$.

- The deflection angle $\Delta\Phi$ of a dipole magnet is related to the path length L_B in the magnet. The trajectory in the external part of the bending magnet ($x > 0$) is slightly more focused since the path length of the particle is longer in the magnetic field, so the deviation $\Delta\phi$ is larger.



- By changing the dipole end's angle to $\varphi < 0$, one can modify the path length L_B in the magnetic field as a function of the horizontal position x :

$$\Delta L_B = -x \tan(\varphi)$$

The dipole exit angle $\varphi < 0$, leads to an increase of the total deflection angle as a function of the transverse position: $\Delta x' = \Delta L_B / R = -x \tan(\varphi) / R$

However, this additive focusing in the horizontal direction results in a defocusing in the vertical plane.

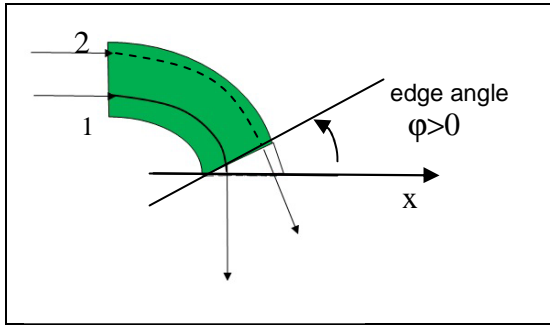


Fig c: Defocusing in horizontal and focusing in vertical plan

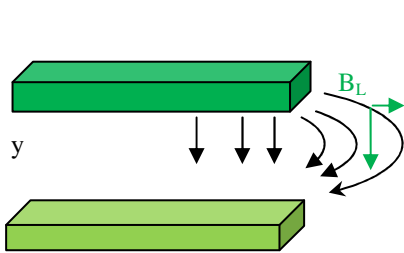
The horizontal defocusing is obvious from the picture, while the vertical focusing needs to be demonstrated (this is related to the field at the end of the dipole, see **Nota**)

c. A dipole edge angle $\varphi > 0$, reduces the path length L_B in the magnetic field as a function of the horizontal position x . The dipole end's angle $\varphi > 0$, leads to a decrease of the total deflection angle as a function of the transverse position x :

$$\Delta x'(2) = \Delta L_B / R = -x \tan(\varphi) / R$$

This defocusing in the horizontal direction is associated with a focusing effect in the vertical plane.

Nota: Let us demonstrate that the inclined edge has some effect the in vertical plane: The inclined edge generates a field component in the horizontal plane due to fringe fields. As seen in the following picture, the end's field connects the south pole to the north pole.



At the exit of the magnet, the field has a longitudinal component B_L .

$$B_L \sim y$$

With $\varphi = 0$, B_L has no effect since v and B_L are perpendicular

If the edge is inclined, the fringe field produces a horizontal component:

$$B_x \sim \sin(\varphi) B_L$$

So $B_x \sim y \sin(\varphi)$ and B_x generate a vertical force:

$$F_y = q (\mathbf{v} \times \mathbf{B})_y = q \cdot v_s \cdot B_x \sim y \sin(\varphi)$$

A bending magnet with an inclined edge ($\varphi > 0$) is often used to control the beam size in the vertical plane with this vertical focusing effect. Entrance and exit inclined edges are often used conjointly.

